RESEARCH ARTICLE

ESPL WILEY

Crustal uplift rates implied by synchronously investigating Late Quaternary marine terraces in the Milazzo Peninsula, Northeast Sicily, Italy

M. Meschis[1] | D. Romano[2] | M. Palano[3,4,5] | G. Scicchitano[6] |
V. De Santis[6] | G. Scardino[6] | A. Gattuso[1] | C. G. Caruso[1] |
F. Sposito[1] | G. Lazzaro[1] | S. S. Sciré Scappuzzo[1] | A. Semprebello[1] |
S. Morici[1] | M. Longo[1]

[1]Istituto Nazionale di Geofisica e Vulcanologia, Sezione di Palermo, Palermo, Italy

[2]Istituto Superiore per la Protezione e la Ricerca Ambientale, Rome, Italy

[3]Department of Earth and Sea Sciences (DiSTeM), University of Palermo, Palermo, Italy

[4]Istituto Nazionale di Geofisica e Vulcanologia, Osservatorio Etneo – Sezione di Catania, Catania, Italy

[5]Consiglio Nazionale Delle Ricerche, Rome, Italy

[6]Department of Earth and Geoenvironmental Sciences, University of Bari, Bari, Italy

Correspondence
M. Meschis, Istituto Nazionale di Geofisica e Vulcanologia, Sezione di Palermo, Via Ugo La Malfa, 153, 90146 Palermo, Italy.
Email: marco.meschis@ingv.it

Abstract

Late Quaternary crustal uplift is well recognized in northeast Sicily, southern Italy, a region also prone to damaging earthquakes such as the 1908 "Messina" earthquake (Mw 7.1), the deadliest seismic event reported within the Italian Earthquake Catalogue. Yet it is still understudied if, within the Milazzo Peninsula, crustal uplift rates are varying spatially and temporally and whether they may be either influenced by (i) local upper-plate faulting activity or (ii) deep geodynamic processes.

To investigate the long-term crustal vertical movements in northeast Sicily, we have mapped a flight of Middle-Late Pleistocene marine terraces within the Milazzo Peninsula and in its southern area and refined their chronology, using a synchronous correlation approach driven by published age controls. This has allowed a new calculation of the associated crustal uplift rates, along a north–south oriented coastal-parallel transect within the investigated area. Our results show a decreasing uplift rate from south to north across the Milazzo Peninsula and beyond, and that the associated rates of uplift have been constant through the Late Quaternary. This spatially varying yet temporally constant vertical deformation helps to constrain the amount of uplift, allowing us to explore which is the driving mechanism(s), proposing a few related scenarios.

We discuss our results in terms of tectonic implications and emphasize the importance of using appropriate approaches, as such applying a synchronous correlation method, to refine chronologies of undated palaeoshorelines when used for tectonic investigations.

KEYWORDS
differential uplift, marine terraces, Milazzo peninsula, uplift rates

1 | INTRODUCTION

A combination of concurrent processes such as crustal uplift, volcanism, continental collision, strike-slip lithospheric faults, subduction process and mantle flow through lithospheric slab windows, along with the associated uncertainty, makes it difficult to properly assess the cause of crustal deformation and the associated rates through time. The herein investigated uplifting Milazzo Peninsula, northeast Sicily in southern Italy, lies within a zone of active continental collision, close to a complex lithospheric strike-slip fault zone, that is, the Aeolian-Tindari-Letojanni Fault System (ATLFS), a distributed dextral transtensional region extending from the back-arc Aeolian Islands (Figure 1) down to the Ionian coast of northeast Sicily (Cultrera, Barreca, Ferranti, et al., 2017b; De Guidi et al., 2013). Middle-Late Pleistocene to Holocene uplift within and close to the investigated area are documented by a preserved flights of palaeoshorelines and tidal
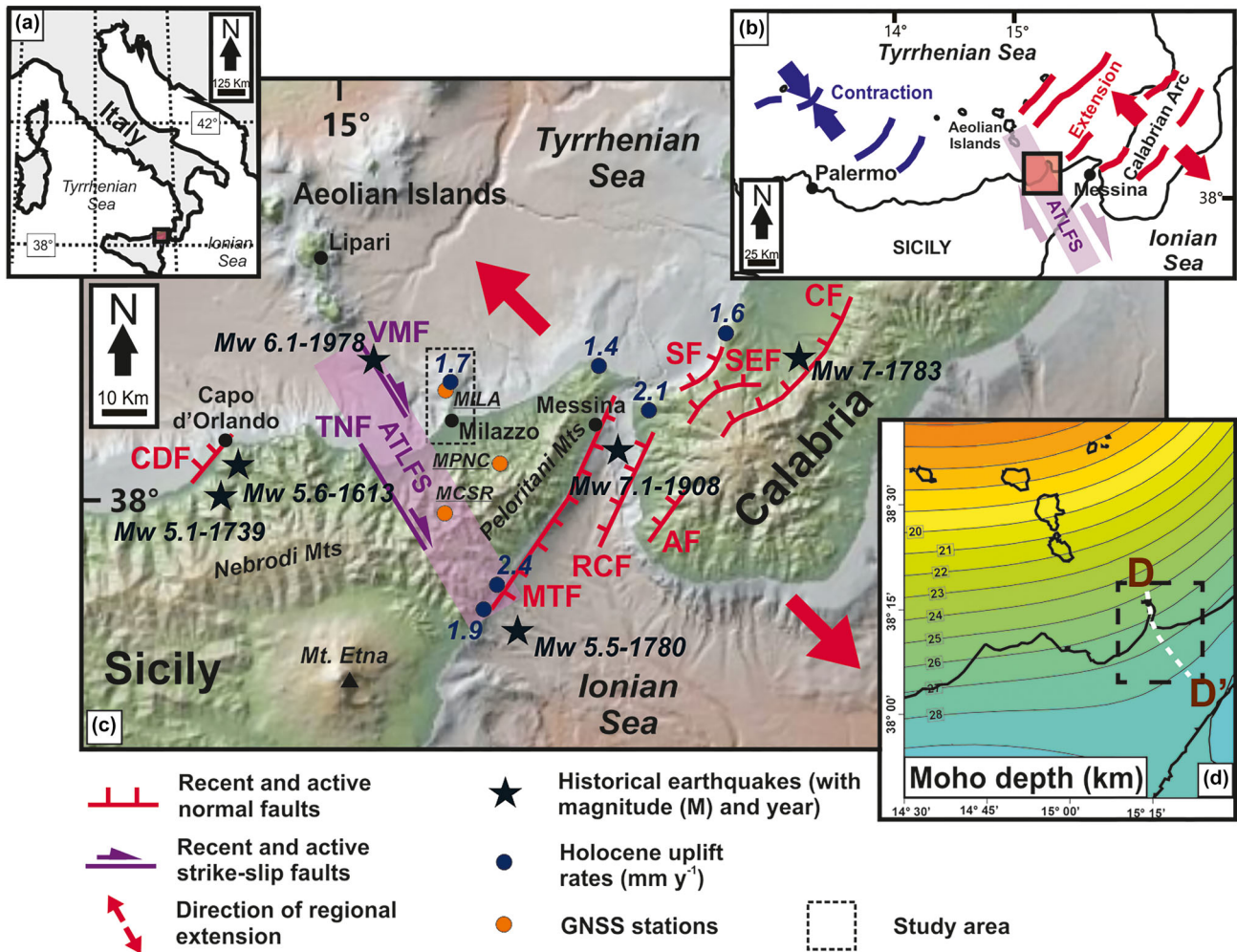
FIGURE 1 Simplified tectonic map of Sicily and Southern Calabria. (a) Inset of Italian territory with location of the investigated area. (b) Inset showing tectonic lineaments and the location of the investigated area; violet, green and red arrows represent compression, lateral and extension crustal deformation, respectively. (c) Red lines represent tectonic faults/lineaments from several previous investigations (e.g. Jacques et al., 2001; Meschis et al., 2018, 2020; Roberts et al., 2013). Red arrows show the direction of regional extension derived by GNSS investigations (Serpelloni et al., 2005). Violet stars show historical seismic events (Rovida et al., 2020). Dark blue squares indicate values of Holocene uplift rates from several investigations (e.g. Antonioli et al., 2006; Scicchitano et al., 2011). Orange circles identify GNSS stations used in this study. Abbreviations are as following: VMF, Vulcano-Milazzo Fault; CF, Cittanova Fault; SF. Scilla Fault; SEF, Sant'Eufemia Fault; MTF, Messina-Taormina Fault; AF, Armo Fault; RCF, Reggio-Calabria Fault; CDF, Capo D'Orlando Fault; TNF, Tindari-Novara Fault; ATLFS, Aeolian-Tindari-Letojanni Fault. (d) Inset showing Moho depth (Grad & Tiira, 2009) beneath northeast Sicily with a dashed white profile trace to study the correlation between uplift rates and Moho depth.

notches (Ferranti et al., 2006; Hearty, 1986; Hearty et al., 1986; Scicchitano et al., 2011). Indeed, a few different uplift scenarios have been debated for the Milazzo Peninsula with uplift rates ranging between ~0.3 and ~0.7 mm/yr (Antonioli et al., 2006; Hearty, 1986; Hearty et al., 1986; Scicchitano et al., 2011), and yet the cause and timing generating Late Quaternary uplift, and its relationship either with the upper-plate faulting or crustal geodynamic processes is still poorly constrained. Additionally, it is still understudied if one or more Quaternary Sea level highstands, identified by the presence of a flight of marine terraces, are preserved and if the associated uplift rates are spatially and temporally changing within the investigated area.

Within the study area, active crustal deformation is also confirmed by the presence of historical seismic events and moderate crustal seismicity with oblique and strike-slip kinematics likely occurring within ATLFS as shown by previous investigations (Barreca et al., 2014; Billi et al., 2006; Frepoli & Amato, 2000; Neri et al., 2005;

Palano et al., 2015; Scicchitano et al., 2011). Indeed, active faulting is implied by the occurrence of historical damaging seismic events with estimated Mw > 6 (e.g. Guidoboni et al., 2019 Jacques et al., 2001; Rovida et al., 2020). Additionally, some authors have proposed that raised Late Holocene tidal notches may be formed as the result of coseismic uplift associated with damaging seismic events of estimated Mw > 6 (Scicchitano et al., 2011). However, it is understudied whether long-term Quaternary crustal uplift affecting the Milazzo Peninsula may be either controlled by active crustal faulting or some subcrustal deep processes associated with the ongoing continental collision/subduction.

The above-mentioned controversies may be addressed and refined rates of crustal uplift over the Quaternary can provide the base for future works leading to a better understanding of tectonic and geodynamic processes controlling the active crustal deformation pattern of the investigated region.

Here, we carry out observations of the raised palaeoshorelines to refine rates of uplift spatially and temporally. Our results are used to discuss if a correlation exists between crustal uplift, subcrustal deep processes associated with the ongoing Africa-Eurasia collision/Ionian subduction process and active crustal faulting.

2 | BACKGROUND

2.1 | Geological and tectonic setting

Northeast Sicily, at the southern edge of the Calabrian-Peloritani Arc, consists of a crustal fragment separated from the Sardinian domain in response to the Neogene evolution of the Ionian subduction system and the opening of the Tyrrhenian Basin (Faccenna et al., 2004; Malinverno & Ryan, 1986). The structural architecture of northeast Sicily (Peloritani Mountains) is characterised by the juxtaposition of different tectonic nappes composed by Variscan crystalline basement rocks discontinuously covered by Meso-Cenozoic sedimentary deposits (Cirrincione et al., 2015). Early Oligocene-Quaternary-aged siliciclastic and carbonate syn- to post-orogenic sedimentary sequences unconformably overlie the nappe edifice (Lentini & Carbone, 2014).

From a tectonic point of view (Figure 1), northeast Sicily is located within the interaction zone between the ~Northwest-Southeast oriented compression occurring along the Sicilian margin of the southern Tyrrhenian Sea (Pondrelli et al., 2004) and the Late Quaternary NW-SE crustal extension affecting the Calabrian-Peloritani Arc (Catalano & De Guidi, 2003; Meschis, Roberts, et al., 2022a; Monaco & Tortorici, 2000), also confirmed by geodetic measurements (D'Agostino et al., 2011; Devoti et al., 2017; Meschis, Teza, et al., 2022b; Palano et al., 2015; Serpelloni et al., 2010). Those

domains are also affected by northnorthwest–southsoutheast trending right-lateral transtensional deformation (ATLFS; Barreca et al., 2014; Billi et al., 2006; Palano et al., 2012) extending from the Vulcano Island to the mainland of Northeast Sicily (Figure 1). GNSS measurements revealed a dextral motion of 3.6 mm/yr occurring along the ATLFS (Palano et al., 2012, 2015). Moreover, this area is marked by a persistent and shallow (depth <40 km) seismicity showing a mixture of normal and oblique focal mechanisms (Palano et al., 2012). The largest earthquakes (i.e. the 1786, Mw = 6.2; 1978, Mw = 6.1, (Rovida et al., 2020) are inferred to have occurred along the major lineaments of the ATLFS (Cultrera, Barreca, Ferranti, et al., 2017a, 2017b).

Although the active deformation pattern of the Tyrrhenian margin of northeast Sicily has been largely investigated over the last few decades (Billi et al., 2006; Cultrera, Barreca, Ferranti, et al., 2017b; De Guidi et al., 2013), only a few historical investigations deal with the structural and geomorphological configuration of the Milazzo Peninsula (Fois, 1990; Lentini et al., 2000), where normal faults, mostly showing Northeast-Southwest trends, were documented. The Variscan basement is widely exposed along the Milazzo Peninsula (Figure 2). It is composed of medium- to high-grade metamorphites including micaschists and migmatitic paragneisses with minor amphibolites and marbles, locally intruded by late Variscan granitoid dykes (D'Amico et al., 1972). Post-orogenic sediments crop out in the northern sector of the Peninsula (Fois, 1990). The oldest sedimentary cycle (Late Miocene) consists of a basal conglomerate horizon formed by crystalline clasts, followed by tens of meters of carbonate edifices surrounded by large breccias derived from the dismantling of the small reef complex. During the Plio-Pleistocene age, yellow and grey marls were deposited within paleo-morphological depressions (Fois, 1990). The top of the sedimentary succession is represented by littoral gravels and pebbly sands indicating a Late Pleistocene sea-level
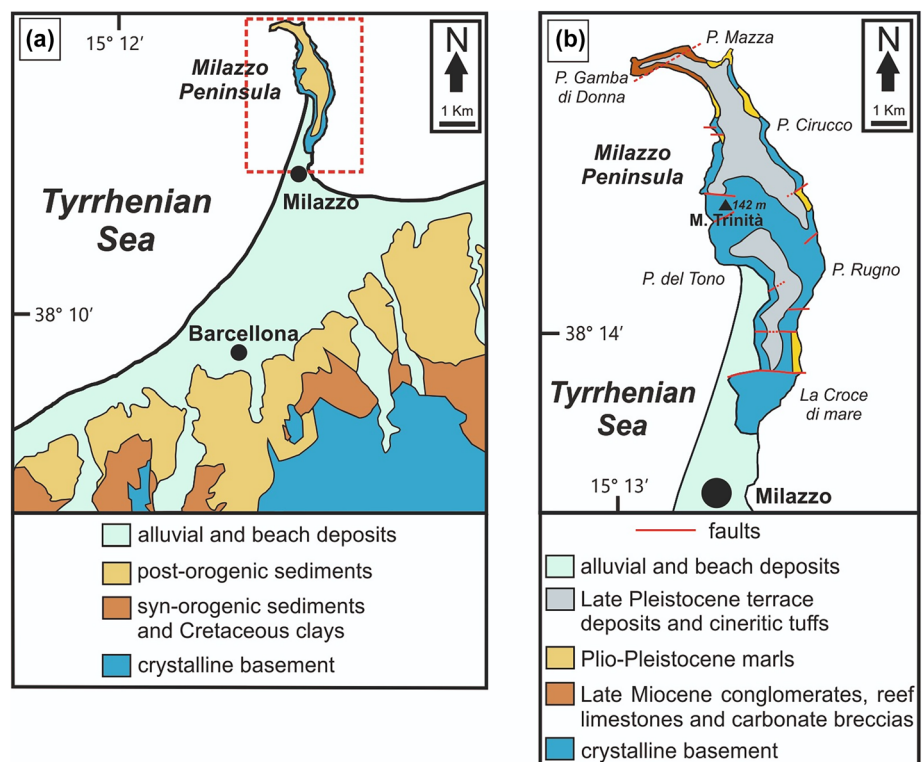

FIGURE 2 Geological maps of the investigated area. (a) A simplified geological map of Milazzo Peninsula (red dashed square) and surrounding area in the south is shown. (b) A more detailed geological map of the Milazzo Peninsula, with red-coloured tectonic lineaments is shown.

highstand, overlaid by cineritic "Brown Tuffs" younger than ∼80 ka, generated by explosive volcanic eruptions likely produced by the Island of Vulcano (Borghi et al., 2014; Lucchi et al., 2008).

2.2 | Late Quaternary uplift in Northeast Sicily

The Ionian subduction beneath the Calabrian-Peloritani Arc is framed in the more general context of the continental collision between Africa and Eurasia plates (Malinverno, 2012), likely controlling the regional uplift recorded in Calabria and northeast Sicily (Gvirtzman & Nur, 1999a, 1999b; Malinverno & Ryan, 1986; Westaway, 1993). In particular, the investigated region lies within the uplifting and seismically extending Calabrian-Peloritani forearc, suggested by the presence of (i) uplifted Quaternary palaeoshorelines and (ii) historical damaging earthquakes (Balescu et al., 1997; Bianca et al., 2011; Cucci et al., 2006; Doglioni et al., 2001; Dumas et al., 1993; Ferranti et al., 2007; Lucente et al., 2006; Miyauchi et al., 1994; Roberts et al., 2013; Stewart et al., 1997; Westaway, 1993). Furthermore, as observed previously, the Calabrian-Peloritani forearc offers prominent geological evidence in the landscape of the interaction between sea-level changes and tectonic uplift processes over the Late Quaternary testified by the presence of sequences of preserved and raised palaeoshorelines (Bianca et al., 2011; Catalano & De Guidi, 2003; Giunta et al., 2012; Pavano et al., 2016; Tortorici et al., 2003; Valensise & Pantosti, 1992). Moreover, the Late Quaternary activity of normal faults accommodating the regional northwest-southeast extensional deformation affects the geometry of preserved palaeoshorelines and the associated crustal uplift rates within both the hangingwall and footwall of active faults (Catalano & De Guidi, 2003; Meschis et al., 2018; Meschis, Roberts, et al., 2022a; Pavano et al., 2016). GNSS measurements confirm crustal deformation with an ongoing active extension and uplift occurring in this area (Chiarabba & Palano, 2017; Mastrolembo Ventura et al., 2014; Serpelloni et al., 2010).

It is important to note that over the last decades, several studies on the Late Quaternary palaeoshorelines outcropping along the Sicilian and Calabrian coasts, identifying the Messina Strait, have been carried out to constrain the crustal uplift (Catalano & De Guidi, 2003; Catalano & Di Stefano, 1997; Meschis et al., 2018; Meschis, Roberts, et al., 2022a; Pavano et al., 2016). Coeval normal faulting over the Late Pleistocene has been affecting the crustal uplift with active faults showing throw-rates ranging between 0.32 and 2.34 mm/yr (Meschis et al., 2018; Meschis, Roberts, et al., 2022a).

Concerning the Milazzo Peninsula, the absence of Senegalese fauna such as *Thetystrombus latus* (also known as *Strombus bubonius*) makes it difficult to identify the elevation of the Marine Isotope Stage (MIS) 5e (125 ka) and the associated uplift rates. For instance, some previous investigations (Hearty, 1986; Hearty et al., 1986) attributed the coarse to sandy deposits, outcropping at elevations between 40 m and 60 m to the 125 ka marker on the basis of aminostratigraphical data collected on *Glycymeris* and *Arca*. This scenario was supported by Bordoni & Valensise (1998). On the other hand, Antonioli et al. (2006) reinterpreted the geomorphological pattern of the Milazzo Peninsula associating the 125 ka highstand to a wide and unique marine terrace occurring at 90 m above the present mean sea level. In addition, two uplifted Holocene palaeoshorelines, represented by tidal notches, marine deposits and balanid rims, take place at ∼2.1 and ∼0.8 m above

the mean sea level (Rust & Kershaw, 2000). According to Scicchitano et al. (2011), the origin of those palaeoshorelines might be linked with abrupt coseismic uplift due to the occurrence of historical major earthquakes (M ∼ 6–7), even though there is no agreement on which fault(s) may have seismically ruptured.

3 | METHODS

In this section, we present methodologies and approaches applied to refine long-term rates of vertical crustal movements within the investigated area of the Milazzo Peninsula.

3.1 | Digital elevation model topographic analysis and palaeoshorelines field mapping

Here, we have followed approaches applied by some previous geoscientists when deformed marine terraces are used to depict tectonic and geodynamic implications within the Mediterranean realm (Meschis et al., 2018, 2020; Meschis, Roberts, et al., 2022a; Meschis, Teza, et al., 2022b; Roberts et al., 2013; Robertson et al., 2019, 2023). In particular, we have carried out detailed geomorphological and topographic analysis by means of both 1 m and 10 m high resolution Digital Elevation Model (DEM) kindly provided by (i) the Italian Ministry of Environment and (ii) TINITALY from INGV (Tarquini et al., 2012), together with field mapping of marine terraces (Figures 3 and 4). Wherever possible, we have mapped prominent breaks of slope identifying inner edges (or shoreline angles) of marine terraces along their strike, both on the DEM and in the field. By using high resolution DEMs, we have traced eight topographic profiles across the current coastline and intercepting flights of marine terraces outcropping on the Milazzo Peninsula and nearby (Figure 3). Note that we have constructed seven topographic profiles (Profile 1–7) on 1 m high resolution DEMs provided by the Italian Ministry of Environment and 1 topographic profile (Profile 8) on 10 m high resolution DEM by TINITALY (Tarquini et al., 2012). The latter has been already used by previous geoscientists for marine terraces investigations assessing its reliability (Meschis et al., 2018; Meschis, Roberts, et al., 2022a; Meschis, Teza, et al., 2022b; Roberts et al., 2013). We have mapped inner edges (or shoreline angles) of marine terraces, which identify glacio-eustatic palaeo mean sea-level associated with warm periods (or highstands from sea level curves) as proposed by some authors in the past (e.g. De Santis et al., 2021, 2023; Ferranti et al., 2021; Jara-Muñoz & Melnick, 2015; Meschis, Teza, et al., 2022b; Robertson et al., 2019, 2023; Saillard et al., 2009) (Figures 3 and 4). It is important to note that topography and GIS-based evidence of palaeoshorelines are used to depict locations of each topographic profile; for example, we have avoided areas affected by fluvial incision produced by the combined action of uplift and river incision to ensure that we have properly studied geomorphological marine (not fluvial) characters. For this reason, our topographic profiles are produced along interfluvial areas where palaeoshorelines are well preserved (Meschis et al., 2020; Meschis et al., 2022b). As shown by previous investigations (De Santis et al., 2021, 2023; Meschis et al., 2020; Meschis, Roberts, et al., 2022a; Meschis, Teza, et al., 2022b; Robertson et al., 2020), field mapping was essential to corroborate (i) our DEM-
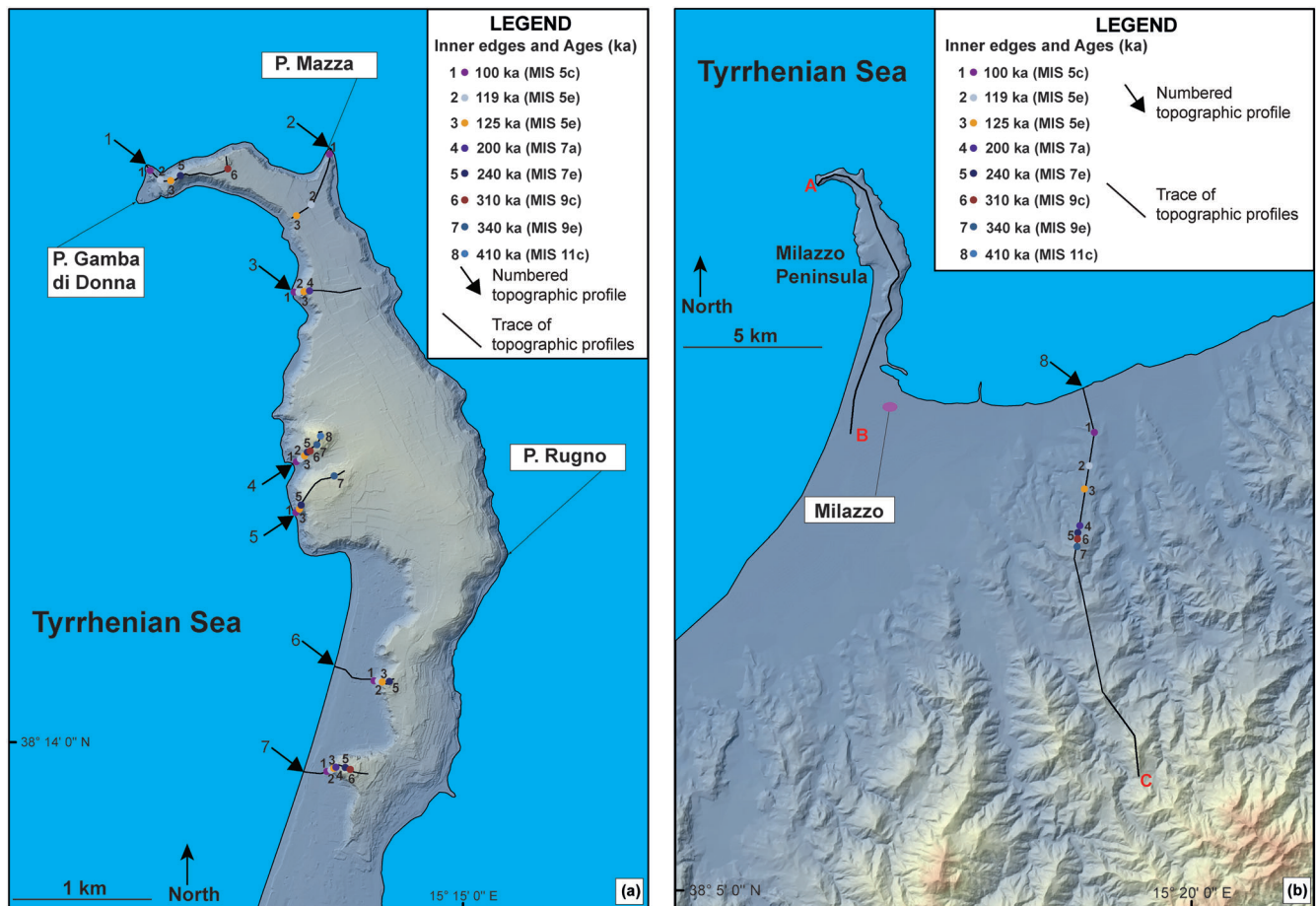
FIGURE 3 Digital terrain models (DTMs) of the study area. (a) A map with locations of serial topographic profiles along the Milazzo Peninsula is shown. Coloured dots represent inner edges of marine terraces and associated refined ages along each serial topographic profile. Serial topographic profiles are constructed on a 1-meter high resolution DTM, kindly provided by "*Regione Siciliana*" government. (b) A map is shown with a location of a serial topographic profile south of Milazzo Peninsula, where a 10-m resolution DTM is used (e.g. Tarquini et al., 2012). Coloured dots represent inner edges of marine terraces and associated refined ages along the topographic profile. Black lines represent the profile used to (i) correlate refined uplift rates and Moho depth and (ii) construct an almost 25 km long topographic profile to show the topography from north to south.

based analysis and (ii) that some palaeoshorelines were less clear on the DEMs to be resolved and mapped (Figure 4); indeed, in places, marine terraces show small palaeo sea cliffs in height updip sloping terraced flat surfaces (a few meters), associated with their limited geographic extent (Figures 3 and 4). In particular, locations of marine terraces are mostly identified as palaeorocky shorelines which are depicted by (i) flat surfaces carved into bedrock by erosion of wave action and in places overlaid by shallow marine deposits lithified by early marine diagenesis (Roberts et al., 2013; Robertson et al., 2019, 2020), (ii) marine erosion pans (also known as millholes) formed by the scouring action of marine pebbles/gravels resulting from the action of sea waves (e.g. Miller & Mason, 1994; Robertson et al., 2019, 2020, 2023) and (iii) caves and lithophagid borings at the updip terminations of wave-cut platforms (Ferranti et al., 2006; Firth & Stewart, 1996; Meschis et al., 2020; Robertson et al., 2019, 2020, 2023). Note that inner edges elevations have been mapped mostly directly on the wave-cut platforms at the junction between the seaward sloping terraced surface and the palaeo-cliff as shown in Figure 4. Yet, it is important to note that in places a few terraced surfaces are overlain by either shallow marine deposits or volcanic deposits, with thicknesses that have been taken into account to derive correct inner edge elevations.

By combining the above-mentioned geomorphological and sedimentary sets of characters, we interpret gently sloping seaward terraced surfaces as palaeoshoreface surfaces carved by the action of sea waves and bounded updip by palaeo sea-cliffs, identifying palaeoshorelines as shown by previous investigations on marine terraces (Armijo et al., 1996; Gallen et al., 2014; Giunta et al., 2012; Meschis et al., 2020; Ott et al., 2019; Pedoja et al., 2018; Roberts et al., 2009, 2013). The dual approach of mapping of palaeoshoreline elevations from fieldwork and DEMs analysis allows us to obtain a wide coverage. Note that our field mapping of palaeoshorelines was corroborated by obtaining topographic elevations using a handheld GPS with a built-in barometric altimeter to constrain palaeoshoreline locations in terms of x, y, and z coordinates as previously proposed by some (Meschis et al., 2018; Roberts et al., 2009, 2013; Robertson et al., 2019, 2023).

3.2 | Ages modelling for undated palaeoshorelines using a synchronous correlation approach

Here, we have applied a synchronous correlation approach that has been largely used and described in the last few decades when marine
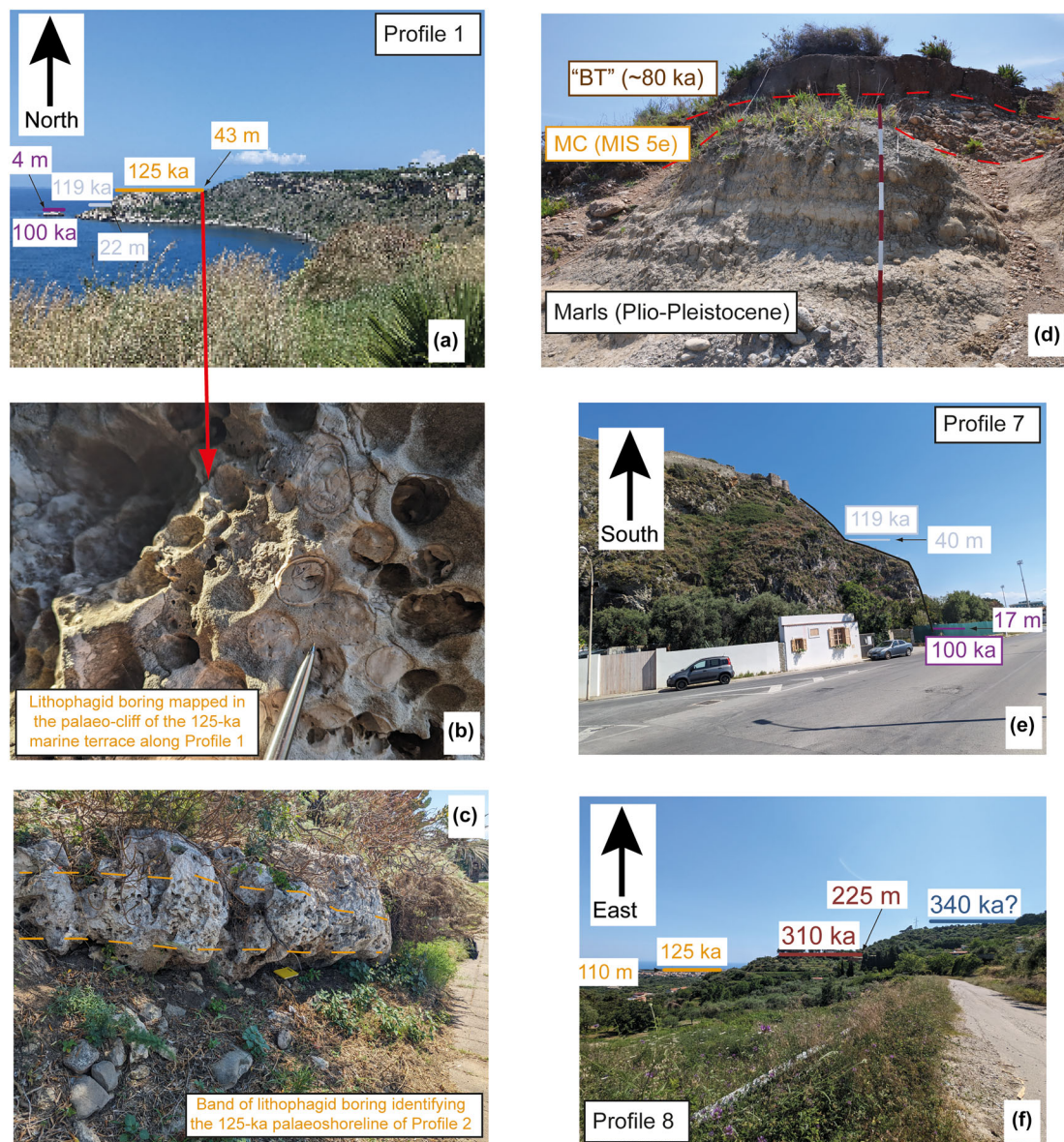
FIGURE 4 Field evidence of our mapped marine terraces. (a) a sequence of marine terraces mapped along Profile 1 in Capo Milazzo, northern part of the investigated area is shown where the MIS 5e (125 ka) at 43 m is mapped. (b) Evidence of lithophagid boring on limestones in places with preserved shelf in Profile 1 suggesting the presence of the palaeo mean sea-level. (c) Evidence of a lithophagid boring "band" on limestones identifying a palaeoshorelines along Profile 2. (d) Sketched stratigraphic sequence in the field close to Capo Milazzo, P. Mazza, where marine deposits belonging to the MIS 5e are overlaid by the younger "Brown Tuff". Location is shown in Figures 1 and 2. (e) A sequence of marine terraces mapped along Profile 7 is shown. (f) A sequence of marine terraces mapped along Profile 8 is shown, south of Milazzo Peninsula and within the Nebrodi-Peloritani chain.

terraces are used to derive tectonic implications and for improved seismic hazard investigations in the Mediterranean realm and elsewhere (De Santis et al., 2021, 2023; Houghton et al., 2003; Meschis et al., 2018, 2020; Meschis, Roberts, et al., 2022a; Meschis, Teza, et al., 2022b; Pedoja et al., 2018; Roberts et al., 2009, 2013; Robertson et al., 2019, 2023). Here, we recall some of its key principles. Indeed, it is built on the concept that glacio-eustatic sea level highstands over the Quaternary are not evenly spaced in time meaning that the consequential raised marine terraces will not be evenly spaced in elevation when an uplift constant through time is hypothesized (Roberts et al., 2009, 2013; Robertson et al., 2019, 2023; Westaway, 1993). It is important to highlight that this approach may be applied when rates of uplift are either constant or fluctuating

through time as discussed by previous investigations (e.g. Meschis, Roberts, et al., 2022a; Roberts et al., 2009, 2013). Furthermore, this method allows us to overcome the problem of assigning erroneous ages to undated palaeoshorelines if the "re-occupation" of older palaeoshorelines by younger ones is not taken into account when relatively slow uplift rates may occur for both constant and fluctuating uplift scenarios (e.g. De Santis et al., 2023; Meschis, Roberts, et al., 2022a; Roberts et al., 2009). This has been recently proved by a study in southern Italy where two raised palaeoshorelines have been numerically dated showing that the older palaeoshoreline associated with the MIS 7c (217 ka) were re-occupied by the younger one associated with the MIS 5e (125 ka) and previously predicted by the synchronous correlation approach (De Santis et al., 2023). Moreover, this

approach is also based on the fact that at least one palaeoshoreline needs to be dated in order to firstly test the simplest hypothesis of a constant uplift rate through time and evaluate the best match between the iteratively calculated sea level highstand elevations and the mapped palaeoshoreline elevations from DEMs and field measurements (De Santis et al., 2021, 2023; Roberts et al., 2009, 2013; Robertson et al., 2019). If a robust correlation is not found for the simplest hypothesised scenario of constant uplift rate through time, then a fluctuating uplift rate scenario is examined, iterating rates of uplift driven by age controls aimed to find the best match between expected and DEM/field mapped palaeoshoreline elevations (e.g. Meschis, Roberts, et al., 2022a; Roberts et al., 2009). It is important to note that we calculate elevations of glacio-eustatic sea-level using well-known Quaternary sea level curves for our marine terrace modelling (Rohling et al., 2014; Siddall et al., 2003) (Table 1), with negligible alterations in terms of uplift rate derivation if different sea-level curves are used (Robertson et al., 2019).

We perform our synchronous correlation between multiple mapped and predicted palaeoshoreline elevations using a "Terrace calculator" built in Excel (Table SI 1) where values of uplift rate (UR) and sea-level highstands are used as input elements (De Santis

et al., 2021, 2023; Meschis et al., 2020; Roberts et al., 2013; Robertson et al., 2019). In particular, by following the formula: $PE = (UR \times T) + SLT$, where T is the age of the highstand and SLT is the sea-level elevation of the highstand relative to the current sea-level position, we calculate PE which is the current predicted elevation of each sea-level highstand (De Santis et al., 2023; Meschis et al., 2020; Meschis, Roberts, et al., 2022a; Meschis, Teza, et al., 2022b). Our outputs from the "Terrace Calculator", a set of predicted palaeoshoreline elevations (PE), are tentatively matched with our mapped palaeoshoreline elevations allowing us to allocate undated palaeoshorelines to sea-level highstands (Meschis et al., 2020; Meschis, Roberts, et al., 2022a; Meschis, Teza, et al., 2022b; Roberts et al., 2013). We stress that iterations of uplift rates have been carried out using the only age control available in literature (Table 2), which suggests that palaeoshorelines mapped between 40 and 60 m in elevations belong to the MIS 5e (125 ka). We then produce linear regression analysis, quantifying the relationship between measured and predicted palaeoshoreline elevations for all the topographic profiles, trying to maximize the coefficient of determination R^2. Finally, we calculate root-mean-square (RMS) deviation to identify the best fit and consequently the best uplift rate value, following an approach already used by some previous investigations (Meschis et al., 2018, 2020; Robertson et al., 2019). In particular, we attempt to obtain accurate values of uplift rates for each topographic profile by iterating uplift rate values from 0 to 1 mm/yr at intervals of 0.05 mm/yr. We then apply the uplift rate values with the lowest RMS deviation to each topographic profile (Figure 5). It is important to note that the margin of error associated with the palaeoshoreline elevations mapped on DEMs is of ± 1 m (Profile 1–7) and ± 10 m (Profile 8). Field measurements were affected by the margin of error associated with the hand-held GPS with values of ±4 m. Regarding the used sea level curves, margin of errors of ± 12 m and 6 m are reported for Siddall et al. (2003) and Rohling et al. (2014) respectively. Margin of errors associated with ages of sea level highstands are of ± 4 kyr for both the sea level curves used in this paper (Rohling et al., 2014; Siddall et al., 2003).

TABLE 1 Sea level highstands values obtained from Siddall et al. (2003) and Rohling et al. (2014) that are used to calculate "predicted" palaeoshoreline elevations by iterating uplift rates driven by age controls.

Age (ka)	Elevation of highstands (mm)
0	0
30	−80,000
50	−60,000
76.5/80	−30,000
100	−25,000
115	−21,000
119	−5,000
125	5,000
175	−30,000
200	−5,000
217	−30,000
240	−5,000
285	−30,000
310	−22,000
340	5,000
410	−5,000
478	0
525	20,000
550	10,000
560	3,000
590	20,000
620	20,000
695	10,000
740	5,000
800	20,000
855	20,000
980	25,000

4 | RESULTS

In this section, we firstly provide evidence that our synchronous correlation approach elucidated in the Methods section permits us to model our mapped elevations of inner edges (or shoreline angle) of marine terraces, identifying palaeoshorelines, by finding the best fit with the predicted and iteratively calculated sea-level highstand elevations. We correlate our mapped palaeoshoreline elevations along the N-S elongated Milazzo Peninsula deriving (i) temporal and spatial constraints associated with the geometry of palaeoshorelines, (ii) related Middle-Late Pleistocene uplift rates and (iii) how these rates are linked with the tectonics of the investigated area.

Table 3 presents all our mapped palaeoshorelines with ages allocated by applying a synchronous correlation technique as shown in Figure 6; note that the table confirms that we were able to corroborate many palaeoshoreline locations mapped on DEMs yet some of them have not been identified in the field because of limited access on private land.

TABLE 2 Age constraints derived from amino acid racemisation (AAR) on Glycymeris and Arca from palaeoshoreline elevations between 40 and 60 m available in the literature. 1 — reference; 2 — dating method; 3 — dated sample description; 4 — profile number; 5 — reported age (kyrs); 6 — assigned Sea-level Highstand (ka); 7 — palaeoshoreline elevations (meters above sea level).

1	2	3	4	5	6	7
Hearty et al., 1986	AAR	*"Using the calibrated amino acid ratios and palaeontological evidence, we correlated the 40–60 m, strandline at Capo Milazzo with the late interglacial Eutyrrhenian or Isotopic Stage 5 … The amino acid data support a last interglacial age for the deposits at Capo Milazzo."*	1,2, 3	100	125	40–60
Lucchi et al., 2008	K/Ar Dating	*"Brown Tuffs occur with thickness up to 12 m at the head of the Capo Milazzo promontory on the northern coast of Sicily. They overlay marine conglomerates attributed to last interglacial on the basis of palaeontology and amino-stratigraphy evidence (135–117 ka; Bordoni & Valensise, 1998, and references therein)."*	1,2, 3	67 ± 8–80	-	40–50

For our synchronous correlation modelling we iterate values of uplift rates to find the best match between multiple palaeoshoreline elevations mapped on DEMs and in the field and multiple predicted sea-level highstand elevations. Following approaches applied by previous investigations using marine terraces (Meschis et al., 2020; Roberts et al., 2013), we have applied two criteria when uplift rates were iterated: (i) we have attempted to correlate the geomorphologically clearest mapped palaeoshorelines with the most prominent sea-level highstands observed in the Mediterranean realm such as the MIS 5e (125 ka), MIS 7e (240 ka) and MIS 9e (340 ka) and, (ii) by linear regression, we have tried to maximize the R^2 value (coefficient of determination) to show the robustness and reliability for other less prominent mapped palaeoshorelines, which have matched the iteratively calculated sea-level highstand elevations such as the MIS 5c (100 ka), MIS 7a (200 ka) and MIS 11c (410 ka). Indeed, this allows us to assign for the first-time ages to previously undated palaeoshorelines along the Milazzo Peninsula as shown in Table 3. Our geomorphological analysis with observations of elevations and locations of palaeoshorelines produced using high resolution DEMs have been assessed to test its robustness and reliability. Indeed, we have carried out linear regression analysis between our DEMs-based mapping and our field observations where the coefficient of determination, R^2, is measured and maximized with values of >0.99 indicating very robust correlation (Figure 7a and b); this suggests that our DEMs-based geomorphological analysis shows a reliable robustness to be used for deriving tectonic implications.

We have also assessed by linear regression analysis our synchronous correlation approach between multiple mapped palaeoshoreline elevations and multiple predicted sea-level highstand elevations (Figure 6 and Table 3). In particular, Figure 7c and d present a prominent correlation with R^2 values >0.99 suggesting that we have gained trustworthy estimates of uplift rates for the investigated area. This is an essential observation because it also indicates that uplift rates mapped along the north–south oriented Milazzo Peninsula have been constant over the Late Quaternary. Note that error bars shown on this regression analysis are allocated taking into account that DEMs have a 1 m resolution and palaeoshoreline elevations mapped in the field have errors of ±4 m associated with the GPS barometric altimeter.

Moreover, we highlight that we have mapped eight orders of marine terraces associated with sea-level highstands between 100 ka and 410 ka, similarly to previous investigations within the Mediterranean realm (De Santis et al., 2021, 2023; Meschis et al., 2018, 2020; Meschis, Roberts, et al., 2022a; Meschis, Teza, et al., 2022b; Roberts et al., 2009, 2013; Robertson et al., 2019, 2023). Note that not all mapped orders of marine terraces, identifying the MIS 5c (100 ka), MIS 5e (119 ka and 125 ka), MIS 7a (200 ka), MIS 7e (240 ka), MIS 9c (310 ka), MIS 9e (340 ka) and MIS 11c (410 ka), have been mapped within a single topographic profile.

Figure 8 shows differential uplift along the north–south oriented Milazzo Peninsula and south of Milazzo town area, recorded by the geometry of the mapped palaeoshorelines (Figure 8a). Consequently, we have derived uplift rates that are constant over time but that change spatially between 0.27 mm/yr in north of the Milazzo Peninsula, increasing towards south where the derived uplift rate is 0.8 mm/yr (Figure 8b). It is important to highlight that the "kink" shown along profiles, between 2 km and 3 km in distance in Figure 8a and b lies within the margin of error associated with the uplift rate values usually up to the 25% of the estimated values (e.g. Meschis et al., 2018; Roberts et al., 2013; Robertson et al., 2019). Furthermore, we have also examined whether the tilting process affected the geometry of palaeoshorelines (Figure 8a) is either coeval or asynchronous to the palaeoshorelines formation. To do that, we have followed an approach proposed by previous studies (Meschis et al., 2018, 2020; Meschis, Roberts, et al., 2022a; Meschis, Teza, et al., 2022b; Roberts et al., 2013; Robertson et al., 2019, 2023) where tilting values of palaeoshorelines are calculated along the north–south oriented Milazzo Peninsula. If the tilting process is coeval to the palaeoshoreline formation, we would hypothesize that older palaeoshorelines should have higher tilting angle values if compared with younger ones. This is confirmed in Figure 8c where higher and older palaeoshorelines show higher tilt angle values suggesting that they have experienced a longer history of crustal deformation with a constant rate through time.

We infer differentially spatially uplifted palaeoshorelines and the temporally changing values of tilting angles as evidence to show crustal deformation with constant rate through time along the investigated north–south oriented Milazzo Peninsula over 25 km.
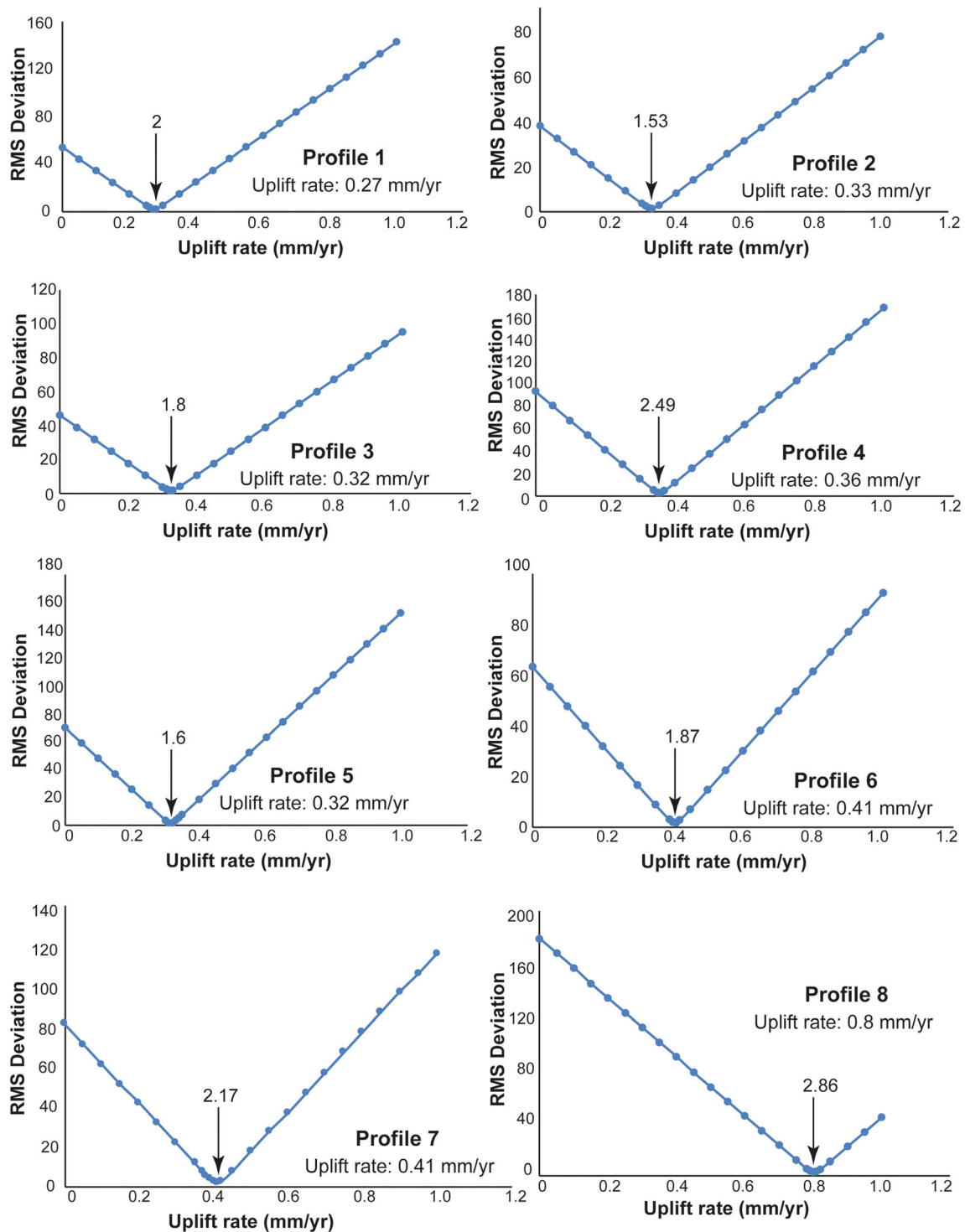
FIGURE 5 Root-mean-square deviation calculation. Root-Mean-Square (RMS) deviation values for all uplifted rate scenarios from 0 to 1.2 mm/yr at intervals of 0.05 mm/yr for each topographic profile. By following previous investigations applying RMS deviation calculations (e.g. Meschis et al., 2020; Robertson et al., 2019), such values unveil the misfit between measured and predicted palaeoshoreline elevations during iteration of the uplift rates, where the lowest RMS misfit is preferred. It shows the best match between "measured" and "predicted" palaeoshorelines elevations. Details of these calculations are shown in Supplementary Material 1.

In the next section, we discuss our results in terms of tectonic implication and which mechanism(s) may be claimed to explain spatially changing yet temporally constant uplift rates within the investigated area.

5 | DISCUSSION

In this paper, our results show a constant uplift rate through time, spanning about the last 0.5 Myr, spatially increasing from north to

TABLE 3 All mapped palaeoshoreline elevations from digital elevation models and fieldwork with age refined by applying a synchronous correlation are shown. 1 — profile number (sea level highstand referred to Figure 3); 2 — UTM coordinate (Easting); 3 — UTM coordinate (Northing); 4 — barometric altimeter palaeoshoreline elevations (this study) (m); 5 — DEMs elevations (m); 6 — predicted elevations (m); 7 — our proposed age (ka).

1	2	3	4	5	6	7
1 (1)	0519664	4,235,783	4	4	2	100
1 (2)	0519731	4,235,724	22	25	27	119
1 (3)	0519807	4,235,712	43	39	39	125
1 (5)	0519891	4,235,750	-	59	60	240
1 (6)	0520203	4,235,792	62	65	62	310
2 (1)	0520937	4,235,882	-	6	8	100
2 (2)	0520795	4,235,528	35	36	34	119
2 (3)	0520676	4,235,451	49	46	46	125
3 (1)	0520685	4,234,918	-	5	7	100
3 (2)	0520715	4,234,912	37	33	33	119
3 (3)	0520723	4,234,912	-	45	45	125
3 (4)	0520742	4,234,919	-	62	59	200
4 (1)	0520708	4,233,722	-	14	11	100
4 (2)	0520730	4,233,734	-	35	38	119
4 (3)	0520738	4,233,742	-	48	50	125
4 (5)	0520769	4,233,781	-	83	81	240
4 (6)	0520777	4,233,790	91	90	90	310
4 (7)	0520848	4,233,850	-	123	127	340
4 (8)	0520862	4,233,901	142	142	143	410
5 (1)	0520700	4,233,362	-	7	7	100
5 (3)	0520714	4,233,385	-	42	45	125
5 (5)	0520732	4,233,415	-	71	72	240
5 (7)	0520982	4,233,619	-	113	114	340
6 (1)	0521263	4,232,164	-	13	16	100
6 (2)	0521306	4,232,152	-	44	44	119
6 (3)	0521313	4,232,149	-	58	56	125
6 (5)	0521350	4,232,146	-	92	93	240
7 (1)	0520933	4,231,524	15	12	13	100
7 (2)	0520955	4,231,535	-	42	45	119
7 (3)	0520966	4,231,542	50	51	53	125
7 (4)	0520975	4,231,548	-	70	71	200
7 (5)	0521046	4,231,549	-	90	86	240
7 (6)	0521060	4,231,540	-	95	96	310
8 (1)	0527262	4,227,791	-	53	55	100
8 (2)	0527044	4,226,722	95	91	90	119
8 (3)	0526859	4,225,907	110	104	105	125
8 (4)	0526676	4,225,101	157	155	150	200
8 (5)	0526604	4,224,780	-	186	187	240
8 (6)	0526575	4,224,654	225	231	226	310
8 (7)	0526540	4,224,499	270	278	277	340

south along the north–south oriented Milazzo Peninsula (Figure 8). In this section, we briefly discuss our results in terms of tectonic implications, possible mechanism that may explain the spatially differential uplift and if there is any kind of correlation between geological and geodetic crustal deformation rates.

5.1 | Possible mechanism(s) controlling the Late Quaternary uplift of the Milazzo Peninsula

Our results show a constant through time yet spatially varying uplift along the north–south oriented Milazzo Peninsula over the Late Quaternary. Here, we discuss some possible mechanism(s) driving the uplift process of the investigated area.

5.1.1 | Upper plate faulting activity

Previous investigations have identified a few active faults that are close and within the investigated area. These include the Capo D'Orlando Fault (Meschis et al., 2018) and the Messina-Taormina Fault (Meschis, Roberts, et al., 2022a) (Figure 1), which have produced a "local" yet prominent vertical deformation consisting of both footwall uplift and hangingwall subsidence over the Late Quaternary. However, the effect of fault deformation decreases with distance from any given fault trace (DeMartini et al., 2004; Ward & Valensise, 1989). Indeed, footwall uplift happens for an across strike distance equivalent to about the half of the fault rupture length (e.g. DeMartini et al., 2004; Meschis et al., 2020; Ward & Valensise, 1989). For instance, the 1983 Borah Peak earthquake (Ms 7.2) generated a coseismic surface rupture of ~30 km along the Lost River Fault, with an associated footwall uplift deformation of ~15 km (Stein & Barrientos, 1985). Similar active faults in terms of their fault geometry (e.g. dip angle, fault activity, etc.) such as the ~ 22 km long Capo D'Orlando Fault and the ~58 km long Messina-Taormina Fault are located approximately 40 and 30–35 km, respectively, from the Milazzo Peninsula. For this reason, we exclude the possibility that the uplift process of the investigated area is influenced by the activity of those faults.

Furthermore, the Milazzo Peninsula lies next to the deep-rooted transtensional ATLFS, which activity is testified by the widespread release at the Earth's surface of mantle-derived fluids (Giammanco et al., 2008; Italiano et al., 2019) and radon (Romano et al., 2023). One may argue that the ATLFS could influence the crustal vertical movement with its activity over the Late Quaternary. However, the prominent component of this fault system is lateral (strike-slip) with no evidence of restraining bends along-strike, and previous investigations have already proved that the effect of the vertical component may be negligible (e.g. Meschis et al., 2019). However, we cannot completely rule out this scenario, since the uplifted Late Holocene paleoshorelines outcropping at Capo Milazzo have been attributed to coseismic deformation by Scicchitano et al. (2011). This is not surprising if we take into account that in other tectonically active regions the overall mechanism(s) of uplift might be more complex, possibly involving unmapped active faults contributing to the uplifted Holocene tidal notches (e.g. Robertson et al., 2023; Scicchitano et al., 2011). For this reason, more investigations are needed to better define if unmapped active faults may play a role for the Late Holocene co-seismic uplift. In particular, we stress that future surveys, focussed on a geochemical approach to assess the role of fluids-related mechanism, have to be taken into account. For instance, measurements of gas fluxes from the soils of the entire Milazzo Peninsula and the surrounding area might unveil buried and/or unknown active faults possibly influencing the vertical crustal movement. Moreover, chemical and isotopic
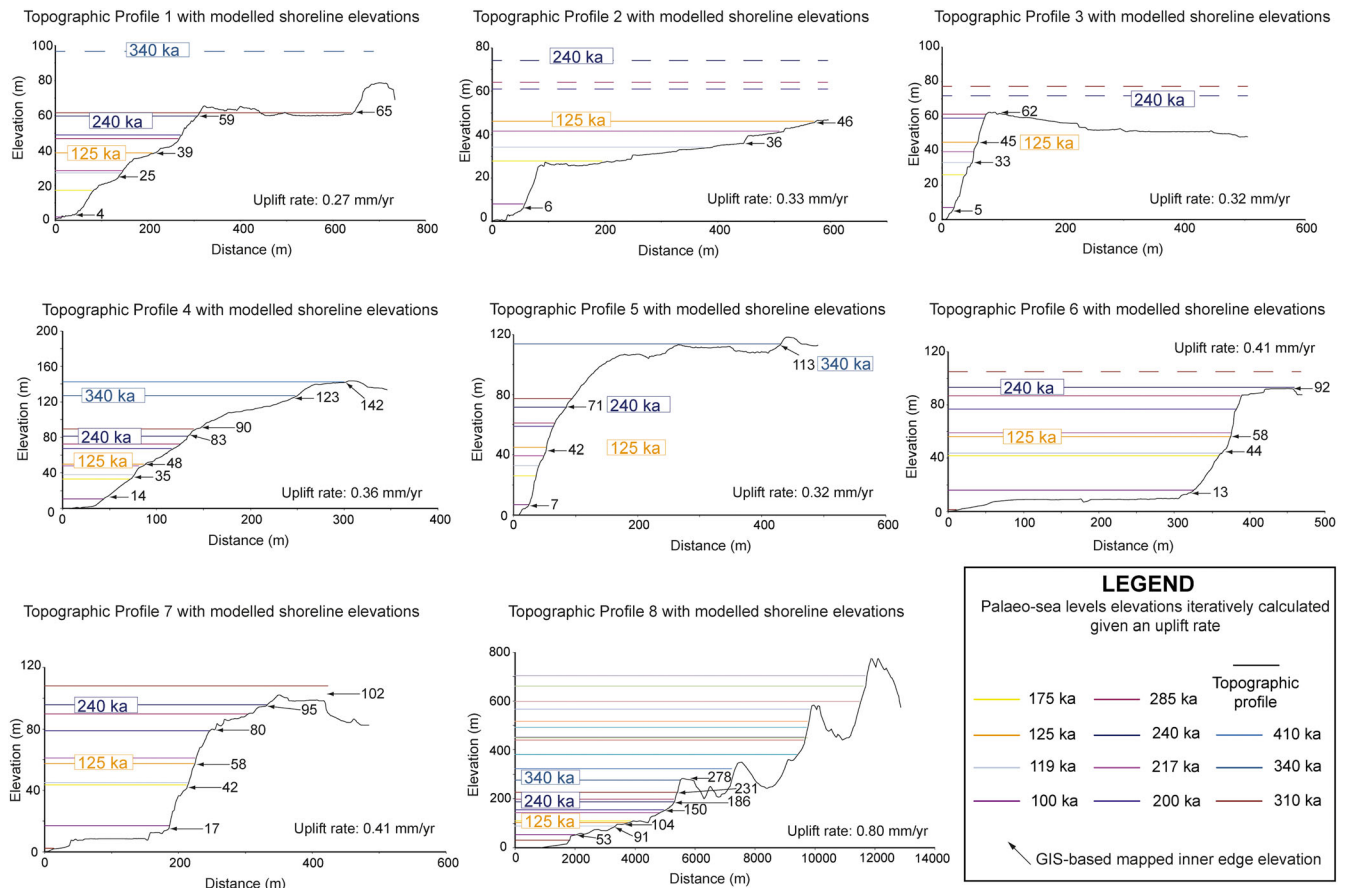
FIGURE 6 Topographic profiles both derived by using (i) 1-m high resolution DTMs for Profile 1-7 and 10-m resolution DEM for Profile 8 (Tarquini et al., 2012) showing mapped and modelled palaeoshoreline elevations. Coloured lines represent the sea-level highstands, which identify the predicted palaeoshoreline elevations, calculated by iterating rates of uplift aimed to find the best fit with the mapped (numbered black arrows) palaeoshorelines. Note that palaeoshoreline elevations are also shown in Table 3.

characterization of released fluids might clarify the input of deep-sourced fluids as a potential engine involved in the differential uplift mechanism.

## 5.1.2 | Regional geodynamic processes

Other explanations for the spatially varying uplift may be related to the Ionian subduction/continental collision and back-arc spreading processes with associated mantle flow around the southeastward retreating Ionian slab (e.g. Barreca et al., 2016; Faccenna, 2011; Faccenna et al., 2004; Lucente et al., 2006; Palano et al., 2017), together with isostatic rebound in response to slab detachment (e.g. Gvirtzman & Nur, 1999a; Neri et al., 2012; Westaway, 1993). Roughly speaking, a slow subduction coupled with mantle upwelling would impose vertical stresses on the overlying crust and may uplift the Earth's surface by hundreds of metres over wavelengths of hundreds to thousands of kilometres (Braun, 2010 and references therein). Such a pattern is clearly observed over the Calabrian Arc, where Meschis et al. (2020) reported an uplift bulge with a wavelength of ∼250–300 km and highest values located along the axial part of the orogenic arc. The uplift pattern observed along the Milazzo Peninsula can be well-framed within the orogenic-related one. We show that higher values of uplift rates are mapped where deeper values of Moho discontinuity depth are depicted (Figure 9a and b).

Furthermore, higher topography with prominent relief energy, defined as the maximum difference in altitude between the peaks and the valley bottoms inside of a defined local space, is mapped where the crust beneath is thicker (Figure 9c). This suggests that crustal thickness may be one of the controlling components of the spatially varying uplift process of the investigated area. This is not surprising if we consider that similar differences in crust thickness (∼4 km) over a few tens kilometres have produced similar spatially varying uplift process in southeast Sicily, with values of uplift rates varying from 0.41 mm/yr to 0.16 mm/yr (Meschis et al., 2020).

Finally, we have also tested whether the uplift process may be controlled by viscous deformation where strain rate (ε) is proportional to the driving stress (σ) raised to an exponent n, which is typically in the range of 2–4 with a power law (Cowie et al., 2013; Mildon et al., 2022). Taking into account a correlation in the form of "$\varepsilon \propto \sigma^n$", we may hypothesize viscous deformation if the driving stress (σ) would be the forces resulting from thick crust raised to an exponent n between 2 and 4 and the strain rate (ε) would be the uplift rate. However, Figure 9d shows that the power law is not well-defined, with the n exponent of 9.9, suggesting that viscous deformations are not the principal control of the spatially varying uplift process.

Based on the considerations here discussed, we suggest therefore that a primary role in driving the observed surface uplift is played by mantle and crustal processes which imposing vertical stresses largely influence the landscape of the study area. The contribute to the
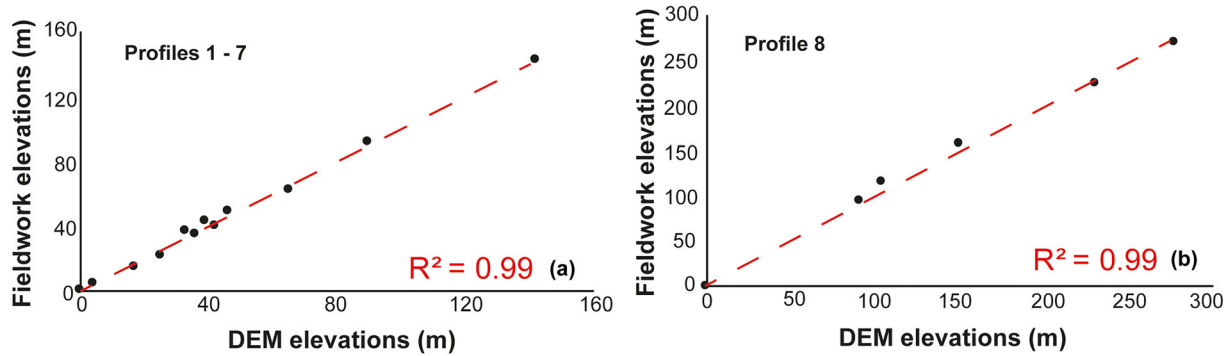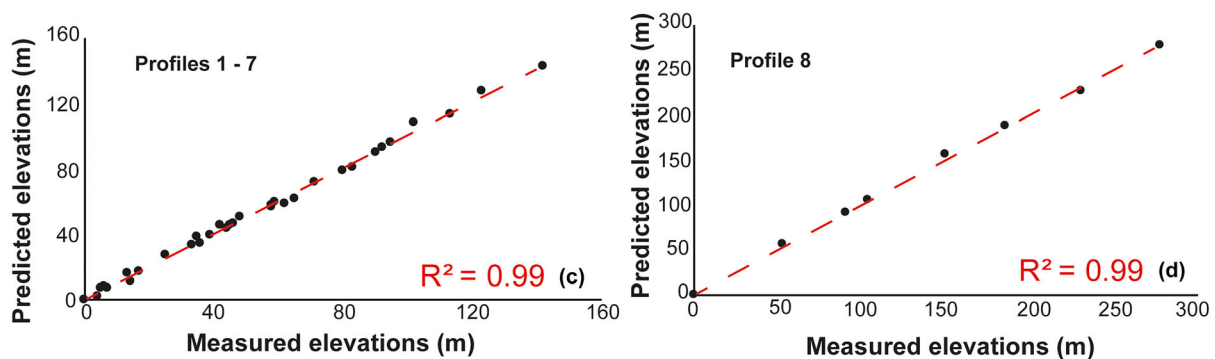
FIGURE 7 Calculation of R^2, coefficient of determination. (a) and (b) correlations between field-based and DEM-based palaeoshoreline elevations are shown by linear regression analysis. (c) and (d) correlations between "measured" and "predicted" palaeoshoreline elevations are shown. It is important to note that "measured" elevations represent palaeoshoreline elevations mapped using DEMs. "Predicted" palaeoshoreline elevations identify the iteratively calculated sea-level highstands by using a synchronous correlation approach and applying a constant uplift rate over the Middle-Late Pleistocene.

surface uplift coming from active faults cutting the study area can be considered as negligible or of small entity.

5.2 | Tectonic implications for the landscape evolution of the Milazzo Peninsula

By applying a synchronous correlation approach, we are able to suggest that a constant uplift rate through time explains the mapped geomorphology in terms of palaeoshoreline elevations and number of palaeoshorelines. In particular, we map a N-S oriented differential uplift with values varying up to four times from 0.27 mm/yr to 0.8 mm/yr along a few tens of kilometres (Figure 8). Indeed, this spatially varying uplift is also confirmed by the tilting process affecting our mapped palaeoshorelines (Figure 8). This suggests that the formation of our mapped palaeoshorelines is temporally coeval with the likely crustal thickening mechanism producing the tilting of the Milazzo Peninsula crust since MIS 11c (410 ka) (Figure 10). This is slightly in contrast with previous investigations where a spatially constant value of ∼0.7 mm/yr along the Milazzo Peninsula (no spatial variations along the north–south oriented peninsula) was proposed (Antonioli et al., 2006).

It is also important to note from our results that an uplift rate value of 0.8 mm/yr is mapped in the Tyrrhenian flank of the Peloritani Mountains (Figure 3b), where palaeoshorelines are carved and preserved in the uplifting northeastern Sicily affected by crustal uplift signal with no "local" upper active faulting influence. This is not surprising if we take into account that similar crustal uplift rate values ranging between 0.89 and 1 mm/yr were mapped where a more "regional" component of uplift is mapped in NE Sicily (Meschis et al., 2018; Meschis, Roberts, et al., 2022a). Furthermore, by combining detailed geomorphological mapping in the field with high-resolution DEMs we identify up to eight09 sea level highstands over 410 ka preserved within the Milazzo Peninsula and south of Milazzo town (not in each topographic profile). This is not surprising if we consider that a similar geomorphology (up to nine mapped palaeoshorelines) and associated spatially varying uplift rates (0.41 to 0.16 mm/yr over a few tens kilometres) were mapped in the relatively tectonically stable SE Sicily (Meschis et al., 2020). Finally, it is also important to note that our youngest mapped palaeoshoreline belongs to the MIS 5c (100 ka). This suggests that our proposed new uplift chronology agrees with the fact that the "Brown Tuffs" deposits, with the base of this rock formation dated 80 ka and where outcropping, are overlying all our older and mapped palaeoshorelines.
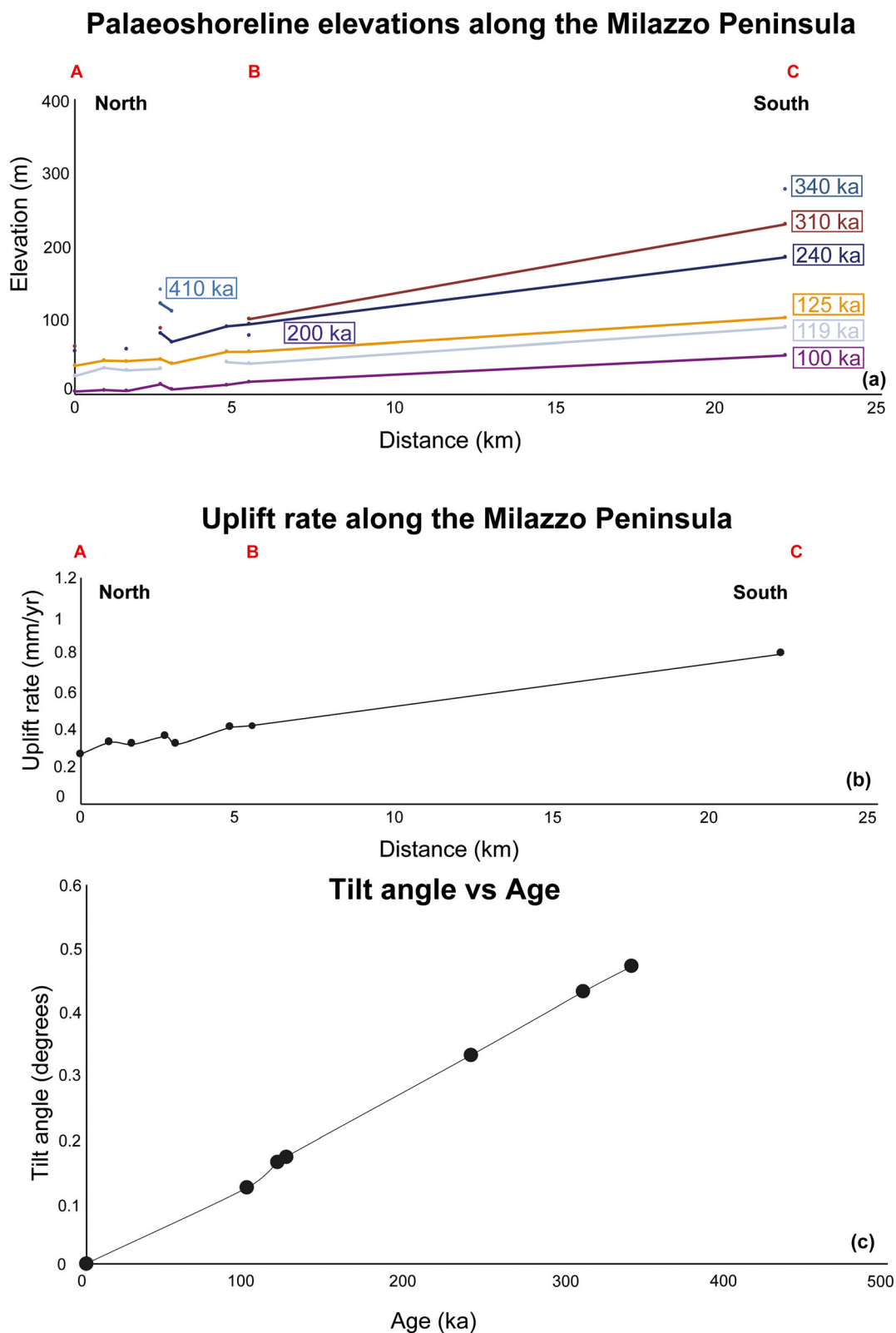
FIGURE 8 (a) Palaeoshoreline elevations tilted along the investigated area (Profile A–C shown in Figure 3b), with ages refined by our modelling shown in Figures 6 and 7 obtained from our topographic profiles. (b) Graph showing how uplift rates derived by applying a synchronous correlation approach (see Figures 6 and 7) change along the investigated area (Profile A–C shown in Figure 3b). (c) Values of tilt angles measured along the investigated area (Profile A–C shown in Figure 3b) showing that tilting process increases with ages for palaeoshorelines, suggesting that their deformation is temporally coeval to the crustal deformation.

These features suggest that after the slowing/cessation of the Ionian subduction/roll-back and the back-arc Tyrrhenian extension (e.g. Goes et al., 2004; Westaway, 1993), the ongoing tectonic reorganization of this sector of the south-central Mediterranean is occurring at constant tectonic rates, at least over the last 0.5 Myr.
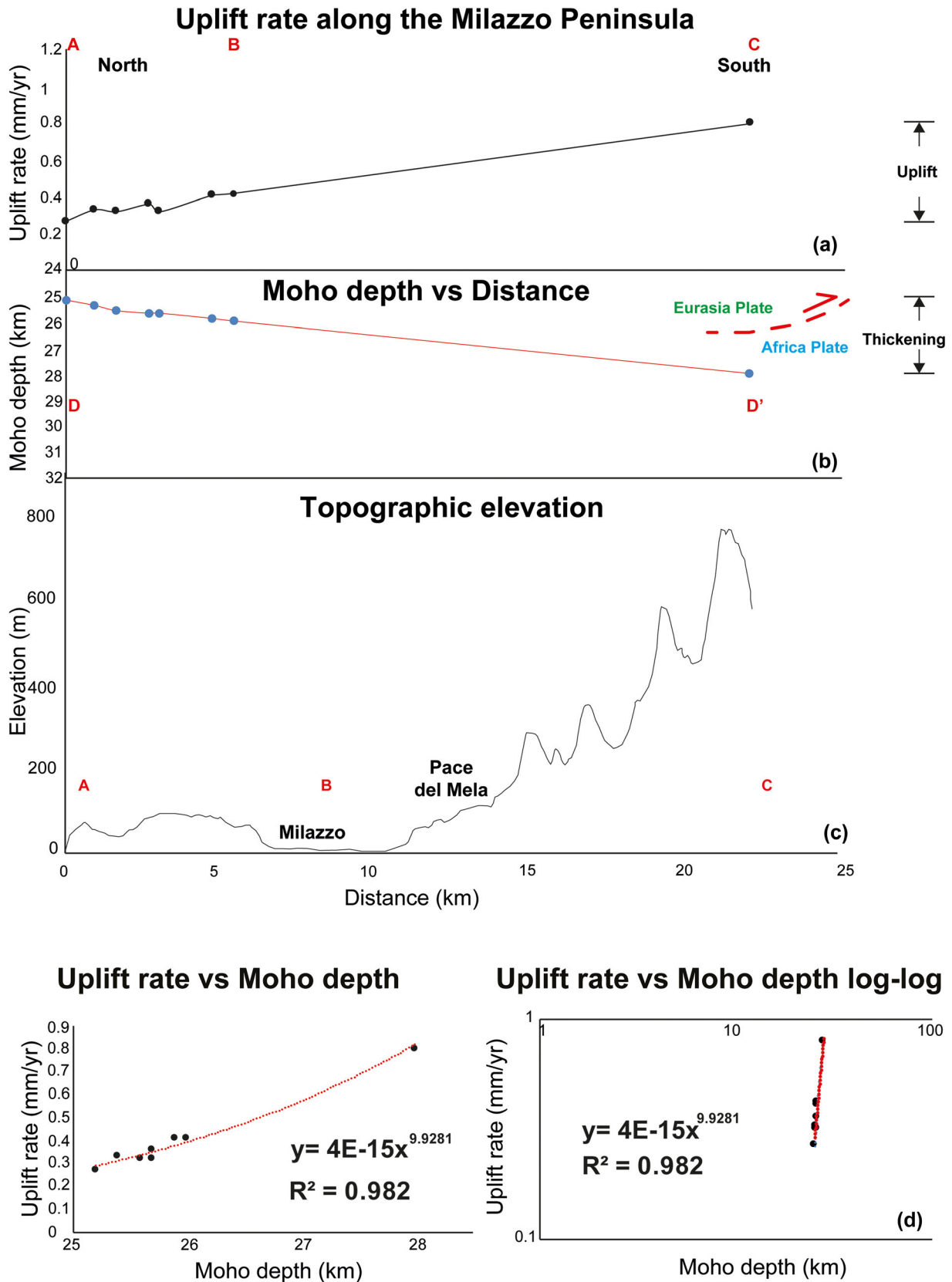
FIGURE 9 (a) Values of uplift rates obtained along the investigated area (profile A-C shown in Figure 3b) shown in the context of crustal thickening (profile D-D′ shown in Figure 1d) (b) and higher energy of relief (higher topography) (c). Note that the continental collision shown in "b" is not scaled. It is important to note that higher uplift rates are mapped where thicker crust is depicted. (d) Correlation between uplift rate and Moho depth. Graphs showing linear regression analysis of Moho depth and uplift rates aimed to test if a power law with an exponent "n" between 2 and 4 which would suggest viscous deformation. However, exponent "n" of 9.9 suggests that a power law for viscous deformation is not well-defined.

FIGURE 10 Not-scaled cartoon showing the temporal evolution of the Milazzo Peninsula with a constant uplift rate through time over the Middle-Late Pleistocene. Location of P. Mazza is where shallow marine deposits belonging to the MIS5e are overlaid by the younger 80 ka-aged "Brown Tuff" as shown in Figure 4d.
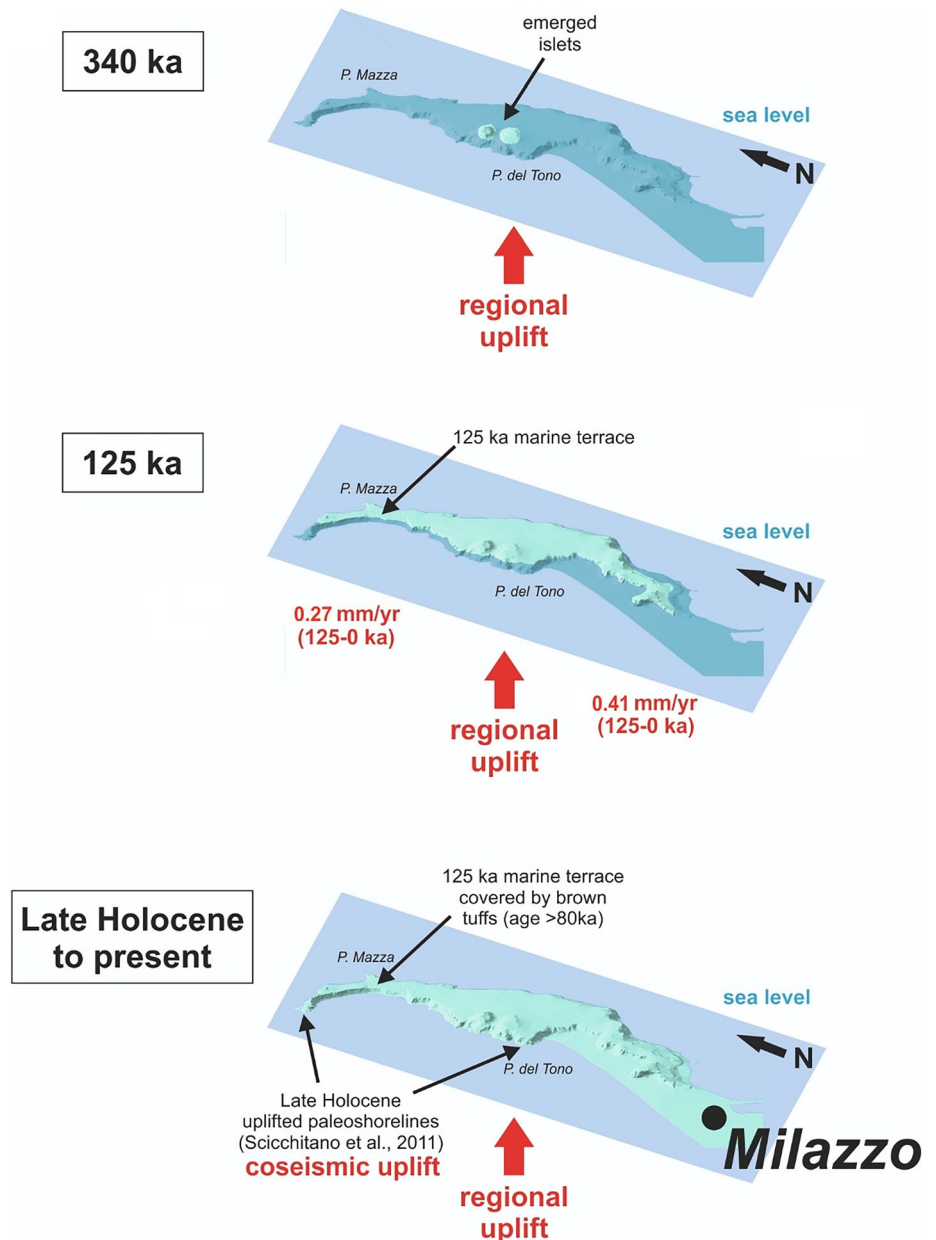
5.3 | Vertical deformation rates at different timescales

In the last decade, estimates of vertical deformation rates for the whole Italian region have been provided by long-term GNSS measurements (Piña-Valdés et al., 2022; Serpelloni et al., 2013). In such a framework the continuous GNSS stations installed on the northern tip of the Milazzo Peninsula (Figure 1) is characterised by a long-term vertical uplift of ca. 0.25 mm/yr (Billi et al., 2023) in good agreement with previous geodetic estimations (Piña-Valdés et al., 2022; Serpelloni et al., 2013) as well as with the geological estimations (0.27 mm/yr over 410 kyrs) performed in this study. Northward, ca. 30 km from the study area, a marked subsidence with rates up to 9.5 mm/yr has been observed for the southernmost sector of the Aeolian Islands. This subsidence would be related to the cumulative effect between a general contraction of local magmatic bodies as recently inferred for the Lipari-Vulcano complex (e.g. Cintorrino et al., 2019 and references therein) and the relative sea level changes

caused by the regional glacio-hydro-isostatic adjustment (Anzidei et al., 2016). Southward, few kilometres from the Milazzo Peninsula (Figure 1), the few available GNSS stations show a subsidence with rates up to 0.7 mm/yr, in contrast with the general uplift of 0.8 mm/yr constrained by the geological data analysed in this study.

Nonetheless, Holocene vertical deformation rates have been proposed by investigating coseismically uplifted tidal notches in Capo Milazzo area, in the northern part of the investigated area in this paper, with an averaged value of 0.65 mm/yr (Scicchitano et al., 2011). This is in contrast with our uplift rate value of 0.27 mm/yr averaged over a longer period of time (few thousand years vs. few hundred thousand years) in the same area.

More in general, our results would stress for more investigations to better understand if a correlation may exist between rates of crustal deformation over the Middle-Late Pleistocene (few hundred thousand years) and those over different and shorter timescales such as the Holocene (few thousand years) in comparison with geodetic ones (few decades). Indeed, the observed discrepancy could be

related to the different time windows identifying short-term (geodetic and Holocene timescales) fluctuations within a long-term (Middle-Late Pleistocene) behaviour.

6 | CONCLUSIONS

In this paper, by applying a synchronous correlation approach we are able to (i) assign ages to undated palaeoshorelines and (ii) refine the uplift chronology, with constant rates through time of the Milazzo Peninsula, in northeast Sicily. In particular, this allows us to show new and improved rates of uplift over the Late Quaternary, overcoming the "overprinting problem" when we investigate regions such as the Milazzo Peninsula affected by relatively low uplift rates. We show that (i) elevations of palaeoshorelines decrease from south to north and (ii) lower uplift rates are mapped in the northern part of the investigated area. Furthermore, we have calculated tilt angle values for raised palaeoshorelines showing higher values for higher and older palaeoshorelines. This suggests that the formation of marine terraces is temporally coeval to the spatially differential uplift of the Milazzo Peninsula. We finally show that highest uplift rates obtained in the southern part of the investigated area are mapped where deeper values of Moho discontinuity are depicted. This suggests that crustal thickness and deep geodynamic processes may be controlling the mapped spatially differential uplift throughout the investigated area.

Finally, our study stresses future works to reconcile crustal deformation rates at different timescales, which may lead to a better (i) understanding of tectonic implications and (ii) assessment of associated seismic hazard for northeast Sicily. Moreover, future works are needed to better understand the relationship between deep geodynamic processes, mantle-derived fluids releasing exploiting potentially active faults and the geomorphology of the NE Sicily. This cannot be carried out if a multidisciplinary approach with geological, geomorphological geochemical and geophysical investigations is not applied.

CONFLICT OF INTEREST STATEMENT

The authors declare no conflict of interest.

DATA AVAILABILITY STATEMENT

The 10-m-resolution Digital Elevation Models data can be freely downloaded at https://tinitaly.pi.ingv.it/, for the analysis on marine terraces and have been properly cited within the manuscript. Furthermore, all data used in this paper are available within this manuscript and the online supplementary material.

ORCID

M. Meschis https://orcid.org/0000-0001-9144-3031
D. Romano https://orcid.org/0000-0002-2122-0737
M. Palano https://orcid.org/0000-0001-7254-7855
G. Scicchitano https://orcid.org/0000-0003-0328-737X
V. De Santis https://orcid.org/0000-0003-0993-0047
G. Scardino https://orcid.org/0000-0002-2316-7888
A. Gattuso https://orcid.org/0000-0003-1815-0421
C. G. Caruso https://orcid.org/0000-0001-5604-0819
F. Sposito https://orcid.org/0000-0001-5063-0965
G. Lazzaro https://orcid.org/0000-0002-0401-0084
S. S. Sciré Scappuzzo https://orcid.org/0000-0002-6554-7758
A. Semprebello https://orcid.org/0000-0001-8690-5254
S. Morici https://orcid.org/0000-0001-9792-9382
M. Longo https://orcid.org/0000-0002-9465-2653

REFERENCES

Antonioli, F., Kershaw, S., Renda, P., Rust, D., Belluomini, G., Cerasoli, M. et al. (2006) Elevation of the last interglacial highstand in Sicily (Italy): a benchmark of coastal tectonics. *Quaternary International*, 145–146, 3–18. Available from: https://doi.org/10.1016/j.quaint.2005.07.002 [online] Available from: https://linkinghub.elsevier.com/retrieve/pii/S1040618205001114

Anzidei, M., Bosman, A., Casalbore, D., Tusa, S. & La Rocca, R. (2016) New insights on the subsidence of Lipari island (Aeolian islands, southern Italy) from the submerged Roman age pier at Marina Lunga. *Quaternary International*, 401, 162–173. Available from: https://doi.org/10.1016/j.quaint.2015.07.003 [online] Available from: https://linkinghub.elsevier.com/retrieve/pii/S1040618215006783 (Accessed 10 January 2024).

Armijo, R., Meyer, B., King, G.C.P., Rigo, A. & Papanastassiou, D. (1996) Quaternary evolution of the Corinth Rift and its implications for the late Cenozoic evolution of the Aegean. *Geophysical Journal International*, 126, 11–53. Available from: https://doi.org/10.1111/j.1365-246X.1996.tb05264.x

Balescu, S., Dumas, B., Guérémy, P., Lamothe, M., Lhénaff, R. & Raffy, J. (1997) Thermoluminescence dating tests of Pleistocene sediments from uplifted marine shorelines along the southwest coastline of the Calabrian peninsula (southern Italy). *Palaeogeography, Palaeoclimatology, Palaeoecology*, 130(1-4), 25–41. Available from: https://doi.org/10.1016/S0031-0182(96)00119-8

Barreca, G., Bruno, V., Cultrera, F., Mattia, M., Monaco, C. & Scarfì, L. (2014) New insights in the geodynamics of the Lipari-Vulcano area (Aeolian archipelago, southern Italy) from geological, geodetic and seismological data. *Journal of Geodynamics*, 82, 150–167. Available from: https://doi.org/10.1016/j.jog.2014.07.003

Barreca, G., Scarfì, L., Cannavò, F., Koulakov, I. & Monaco, C. (2016) New structural and seismological evidence and interpretation of a lithospheric-scale shear zone at the southern edge of the Ionian subduction system (Central-Eastern Sicily, Italy). *Tectonics*, 35(6), 1489–1505. Available from: https://doi.org/10.1002/2015TC004057

Bianca, M., Catalano, S., De Guidi, G., Gueli, A.M., Monaco, C., Ristuccia, G.M. et al. (2011) Luminescence chronology of Pleistocene marine terraces of capo Vaticano peninsula (Calabria, southern Italy).

Quaternary International, 232(1-2), 114–121. Available from: https://doi.org/10.1016/j.quaint.2010.07.013 [online] Available from: http://linkinghub.elsevier.com/retrieve/pii/S1040618210002788 (Accessed 10 October 2014).

Billi, A., Cuffaro, M., Orecchio, B., Palano, M., Presti, D. & Totaro, C. (2023) Retracing the Africa–Eurasia nascent convergent boundary in the western Mediterranean based on earthquake and GNSS data. *Earth and Planetary Science Letters*, 601, 117906. Available from: https://doi.org/10.1016/j.epsl.2022.117906 [online] Available from: https://linkinghub.elsevier.com/retrieve/pii/S0012821X22005428 (Accessed 9 January 2024).

Billi, A., Porreca, M., Faccenna, C. & Mattei, M. (2006) Magnetic and structural constraints for the noncylindrical evolution of a continental forebulge (Hyblea, Italy). *Tectonics*, 25(3). Available from: https://doi.org/10.1029/2005TC001800

Bordoni, P. & Valensise, G. (1998) Deformation of the 125 ka marine terrace in Italy: tectonic implications. *Geological Society, London, Special Publications*, 146(1), 71–110. Available from: https://doi.org/10.1144/GSL.SP.1999.146.01.05

Borghi, E., Garilli, V. & Bonomo, S. (2014) Plio-Pleistocene Mediterranean bathyal echinoids: evidence of adaptation to psychrospheric conditions and affinities with Atlantic assemblages. *Palaeontologia Electronica*, Available from: https://doi.org/10.26879/476 [online] Available from: http://palaeo-electronica.org/content/2014/979-cenozoic-deep-water-echinoids (Accessed 22 January 2024).

Braun, J. (2010) The many surface expressions of mantle dynamics. *Nature Geoscience*, 3(12), 825–833. Available from: https://doi.org/10.1038/ngeo1020 [online] Available from: https://www.nature.com/articles/ngeo1020 (Accessed 21 May 2024).

Catalano, S. & De Guidi, G. (2003) Late Quaternary uplift of northeastern Sicily: relation with the active normal faulting deformation. *Journal of Geodynamics*, 36(4), 445–467. Available from: https://doi.org/10.1016/S0264-3707(02)00035-2

Catalano, S. & Di Stefano, A. (1997) Sollevamenti e tettogenesi pleistocenica lungo il margine tirrenico dei Monti Peloritani: integrazione dei dati geomorfologici, strutturali e biostratigrafici. *Il Quaternario*, 10, 337–342.

Chiarabba, C. & Palano, M. (2017) Progressive migration of slab break-off along the southern Tyrrhenian plate boundary: constraints for the present day kinematics. *Journal of Geodynamics*, 105, 51–61. Available from: https://doi.org/10.1016/j.jog.2017.01.006 [online] Available from: http://www.sciencedirect.com/science/article/pii/S0264370716300485

Cintorrino, A.A., Palano, M. & Viccaro, M. (2019) Magmatic and tectonic sources at Vulcano (Aeolian Islands, southern Italy): a geodetic model based on two decades of GPS observations. *Journal of Volcanology and Geothermal Research*, 388, 106689. Available from: https://doi.org/10.1016/j.jvolgeores.2019.106689 [online] Available from: https://linkinghub.elsevier.com/retrieve/pii/S0377027319303762 (Accessed 10 January 2024).

Cirrincione, R., Fazio, E., Fiannacca, P., Ortolano, G., Pezzino, A. & Punturo, R. (2015) The Calabria-Peloritani Orogen, a composite terrane in Central Mediterranean; its overall architecture and geodynamic significance for a pre-Alpine scenario around the Tethyan basin. *Periodico di Mineralogia*, 84, 701–749. Available from: https://doi.org/10.2451/2015PM0446

Cowie, P.A., Scholz, C.H., Roberts, G.P., Faure Walker, J.P. & Steer, P. (2013) Viscous roots of active seismogenic faults revealed by geologic slip rate variations. *Nature Geoscience*, 3, 10–14. Available from: https://doi.org/10.1038/ngeo1991

Cucci, L., Tertulliani, A., Nazionale, I., Sismologia, S. & Murata, V. (2006) I Terrazzi Marini Nell' Area Di Capo Vaticano (Arco Calabro): Solo Un Record Di Sollevamento Regionale O Anche Di Deformazione Cosismica ? *Il Quaternario*, 19, 89–101.

Cultrera, F., Barreca, G., Burrato, P., Ferranti, L., Monaco, C., Passaro, S. et al. (2017a) Active faulting and continental slope instability in the gulf of patti (Tyrrhenian side of NE sicily, Italy): a field, marine and seismological joint analysis. *Natural Hazards*, 86(S2), S253–S272. Available from: https://doi.org/10.1007/s11069-016-2547-y

Cultrera, F., Barreca, G., Ferranti, L., Monaco, C., Pepe, F., Passaro, S. et al. (2017b) Structural architecture and active deformation pattern in the northern sector of the Aeolian-Tindari-Letojanni fault system (SE Tyrrhenian Sea-NE Sicily) from integrated analysis of field, marine geophysical, seismological and geodetic data. *Italian Journal of Geosciences*, 136(3), 399–417. Available from: https://doi.org/10.3301/IJG.2016.17 [online] Available from: http://www.italianjournalofgeosciences.it/244/fulltext.html?ida=838

D'Agostino, N., D'Anastasio, E., Gervasi, A., Guerra, I., Nedimović, M.R., Seeber, L. et al. (2011) Forearc extension and slow rollback of the Calabrian arc from GPS measurements. *Geophysical Research Letters*, 38(17). Available from: https://doi.org/10.1029/2011GL048270

D'amico, C., Gurrieri, S. & Maccarrone, E. (1972) Le Metamorfiti di Milazzo (Messina). *Periodico di Mineralogia*, 41, 35–141.

De Guidi, G., Lanzafame, G., Palano, M., Puglisi, G., Scaltrito, A. & Scarfi, L. (2013) Multidisciplinary study of the Tindari fault (Sicily, Italy) separating ongoing contractional and extensional compartments along the active Africa–Eurasia convergent boundary. *Tectonophysics*, 588, 1–17. Available from: https://doi.org/10.1016/j.tecto.2012.11.021

De Santis, V., Scardino, G., Meschis, M., Ortiz, J.E., Sánchez-Palencia, Y. & Caldara, M. (2021) Refining the middle-late Pleistocene chronology of marine terraces and uplift history in a sector of the Apulian foreland (southern Italy) by applying a synchronous correlation technique and amino acid racemization to patella spp. and Thetystrombus latus. *Italian Journal of Geosciences*, 140(3), 438–463. Available from: https://doi.org/10.3301/IJG.2021.05 [online] Available from: https://www.italianjournalofgeosciences.it/297/article-1107/refining-the-middle-late-pleistocene-chronology-of-marine-terraces-and-uplift-history-in-a-sector-of-the-apulian-foreland-southern-italy-by-applying-a-synchronous-correlation-technique-and-amino-

De Santis, V., Scardino, G., Scicchitano, G., Meschis, M., Montagna, P., Pons-Branchu, E. et al. (2023) Middle-late Pleistocene chronology of palaeoshorelines and uplift history in the low-rising to stable Apulian foreland: overprinting and reoccupation. *Geomorphology*, 421, 108530. Available from: https://doi.org/10.1016/j.geomorph.2022.108530 [online] Available from: https://linkinghub.elsevier.com/retrieve/pii/S0169555X22004238

DeMartini, P.M., Pantosti, D., Palyvos, N., Lemeille, F., McNeill, L. & Collier, R. (2004) Slip rates of the Aigion and Eliki faults from uplifted marine terraces, Corinth gulf, Greece. *Comptes Rendus Geoscience*, 336(4-5), 325–334. Available from: https://doi.org/10.1016/j.crte.2003.12.006 [online] Available from: https://linkinghub.elsevier.com/retrieve/pii/S1631071304000161

Devoti, R., D'Agostino, N., Serpelloni, E., Pietrantonio, G., Riguzzi, F., Avallone, A. et al. (2017) A combined velocity field of the Mediterranean region. *Annals of Geophysics*, 60(2), S0215. Available from: https://doi.org/10.4401/ag-7059 [online] Available from: http://www.annalsofgeophysics.eu/index.php/annals/article/view/7059 (Accessed 30 April 2017).

Doglioni, C., Innocenti, F. & Mariotti, G. (2001) Why Mt Etna ? *Terra Nova*, 13(1), 25–31. Available from: https://doi.org/10.1046/j.1365-3121.2001.00301.x

Dumas, B., Gueremy, P., Lhenaff, R. & Raffy, J. (1993) Rapid uplift, stepped marine terraces and raised shorelines on the Calabrian coast of Messina Strait, Italy. *Earth Surface Processes and Landforms*, 18(3), 241–256. Available from: https://doi.org/10.1002/esp.3290180306

Faccenna, C. (2011) Topography of the Calabria subduction zone (southern Italy): clues for the origin of Mt. Etna. 30(1), Available from: https://doi.org/10.1029/2010TC002694

Faccenna, C., Piromallo, C., Crespo-Blanc, A., Jolivet, L. & Rossetti, F. (2004) Lateral slab deformation and the origin of the western Mediterranean arcs. *Tectonics*, 23: n/a-n/a, Available from: https://doi.org/10.1029/2002TC001488 (Accessed 17 February 2016).

Ferranti, L., Antonioli, F., Mauz, B., Amorosi, A., Dai Pra, G., Mastronuzzi, G. et al. (2006) Markers of the last interglacial sea-level high stand along the coast of Italy: tectonic implications. *Quaternary International*, 145–146, 30–54. Available from: https://doi.org/10.1016/j.quaint.2005.07.009 [online] Available from: http://linkinghub.elsevier.com/retrieve/pii/S1040618205001138 (Accessed 18 October 2014).

Ferranti, L., Burrato, P., Sechi, D., Andreucci, S., Pepe, F. & Pascucci, V. (2021) Late Quaternary coastal uplift of southwestern Sicily, Central Mediterranean Sea. *Quaternary Science Reviews*, 255, 106812. Available from: https://doi.org/10.1016/j.quascirev.2021.106812

Ferranti, L., Monaco, C., Antonioli, F., Maschio, L., Kershaw, S. & Verrubbi, V. (2007) The contribution of regional uplift and coseismic slip to the vertical crustal motion in the Messina Straits, southern Italy: evidence from raised Late Holocene shorelines. *Journal of Geophysical Research*, 112(B6), B06401. Available from: https://doi.org/10.1029/2006JB004473

Firth, C. & Stewart, I. (1996) Coastal elevation changes in eastern Sicily: implications for volcano instability at Mount Etna. *Geological Society*, (1), 153–167. Available from: https://doi.org/10.1144/GSL.SP.1996.110.01.12

Fois, E. (1990) Stratigraphy and palaeogeography of the capo Milazzo area (NE Sicili, Italy): clues to the evolution of the southern margin of the Tyrrhenian Basin during the Neogene. *Palaeogeography, Palaeoclimatology, Palaeoecology*, 78(1-2), 87–108. Available from: https://doi.org/10.1016/0031-0182(90)90206-M [online] Available from: https://linkinghub.elsevier.com/retrieve/pii/003101829090206M

Frepoli, A. & Amato, A. (2000) Spatial variation in stresses in peninsular Italy and Sicily from background seismicity. *Tectonophysics*, 317(1-2), 109–124. Available from: https://doi.org/10.1016/S0040-1951(99)00265-6 [online] Available from: https://linkinghub.elsevier.com/retrieve/pii/S0040195199002656

Gallen, S.F., Wegmann, K.W., Bohnenstiehl, D.R., Pazzaglia, F.J., Brandon, M.T. & Fassoulas, C. (2014) Active simultaneous uplift and margin-normal extension in a forearc high, Crete, Greece. *Earth and Planetary Science Letters*, 398, 11–24. Available from: https://doi.org/10.1016/j.epsl.2014.04.038

Giammanco, S., Palano, M., Scaltrito, A., Scarfì, L. & Sortino, F. (2008) Possible role of fluid overpressure in the generation of earthquake swarms in active tectonic areas: the case of the Peloritani Mts. (Sicily, Italy). *Journal of Volcanology and Geothermal Research*, 178(4), 795–806. Available from: https://doi.org/10.1016/j.jvolgeores.2008.09.005 [online] Available from: https://linkinghub.elsevier.com/retrieve/pii/S037702730800485X (Accessed 9 January 2024).

Giunta, G., Gueli, A.M., Monaco, C., Orioli, S., Ristuccia, G.M., Stella, G. et al. (2012) Middle-Late Pleistocene marine terraces and fault activity in the Sant'Agata di Militello coastal area (North-Eastern Sicily). *Journal of Geodynamics*, 55, 32–40. Available from: https://doi.org/10.1016/j.jog.2011.11.005

Goes, S., Giardini, D., Jenny, S., Hollenstein, C., Kahle, H.-G. & Geiger, A. (2004) A recent tectonic reorganization in the south-Central Mediterranean. *Earth and Planetary Science Letters*, 226(3-4), 335–345. Available from: https://doi.org/10.1016/j.epsl.2004.07.038 [online] Available from: http://linkinghub.elsevier.com/retrieve/pii/S0012821X04004741

Grad, M. & Tiira, T. (2009) The Moho depth map of the European plate. *Geophysical Journal International*, 176(1), 279–292. Available from: https://doi.org/10.1111/j.1365-246X.2008.03919.x

Guidoboni, E., Ferrari, G., Tarabusi, G., Sgattoni, G., Comastri, A., Mariotti, D. et al. (2019) CFTI5Med, the new release of the catalogue of strong earthquakes in Italy and in the Mediterranean area. *Scientific Data*, 6(1), 80. Available from: https://doi.org/10.1038/s41597-019-0091-9

Gvirtzman, Z. & Nur, A. (1999a) Plate detachment, asthenosphere upwelling, and topography across subduction zones. *Geology*, 27(6), 563. Available from: https://doi.org/10.1130/0091-7613(1999)027<0563:PDAUAT>2.3.CO;2

Gvirtzman, Z. & Nur, A. (1999b) The formation of Mount Etna as the consequence of slab rollback. *Nature*, 401(6755), 782–785. Available from: https://doi.org/10.1038/44555

Hearty, P.J. (1986) An inventory of last interglacial (sensu lato) age deposits from the Mediterranean Basin: a study of isoleucine epimerization and U-series dating. *Zeitschrift für Geomorphologie, Supplementary Issues*, 62, 51–69.

Hearty, P.J., Bonfiglio, L., Violanti, D. & Szabo, B. (1986) Age of late Quaternary marine deposits of southern Italy determined by aminostratigraphy, faunal correlation, and uranium-series dating. *Revista Italiana di Paleontologia e Stratigraphia*, 92, 149–164.

Houghton, S.L., Roberts, G.P., Papanikolaοu, I.D. & McArthur, J.M. (2003) New 234 U- 230 Th coral dates from the western gulf of Corinth: implications for extensional tectonics. *Geophysical Research Letters*, 30(19), 2013. Available from: https://doi.org/10.1029/2003GL018112 [online] Available from: http://discovery.ucl.ac.uk/546/

Italiano, F., Bonfanti, P. & Maugeri, S.R. (2019) Evidence of tectonic control on the geochemical features of the volatiles vented along the Nebrodi-Peloritani Mts (southern Apennine chain, Italy). *Geofluids*, 2019, 1–17. Available from: https://doi.org/10.1155/2019/6250393 [online] Available from: https://www.hindawi.com/journals/geofluids/2019/6250393/ (Accessed 9 January 2024).

Jacques, E., Monaco, C., Tapponnier, P., Tortorici, L. & Winter, T. (2001) Faulting and earthquake triggering during the 1783 Calabria seismic sequence. *Geophysical Journal International*, 147(3), 499–516. Available from: https://doi.org/10.1046/j.0956-540x.2001.01518.x

Jara-Muñoz, J. & Melnick, D. (2015) Unraveling Sea-level variations and tectonic uplift in wave-built marine terraces, Santa María Island, Chile. *Quaternary Research*, 83(1), 216–228. Available from: https://doi.org/10.1016/j.yqres.2014.10.002 [online] Available from: http://linkinghub.elsevier.com/retrieve/pii/S0033589414001276

Lentini, F. & Carbone, S. (2014) Geologia della Sicilia-geology of Sicily. *Memorie Descrittive Della Carta Geologica d'Italia*, 95, 7–414.

Lentini F, Carbone S, Catalano S. 2000. *Carta Geologica della Provincia di Messina*.

Lucchi, F., Tranne, C.A., De Astis, G., Keller, J., Losito, R. & Morche, W. (2008) Stratigraphy and significance of Brown tuffs on the Aeolian Islands (southern Italy). *Journal of Volcanology and Geothermal Research*, 177(1), 49–70. Available from: https://doi.org/10.1016/j.jvolgeores.2007.11.006

Lucente, F.P., Margheriti, L., Piromallo, C. & Barruol, G. (2006) Seismic anisotropy reveals the long route of the slab through the western-Central Mediterranean mantle. *Earth and Planetary Science Letters*, 241(3-4), 517–529. Available from: https://doi.org/10.1016/j.epsl.2005.10.041 [online] Available from: http://linkinghub.elsevier.com/retrieve/pii/S0012821X05008083

Malinverno, A. (2012) *Evolution of the Tyrrhenian Sea-Calabrian arc system: the past and the present*, pp. 11–15.

Malinverno, A. & Ryan, W.B.F. (1986) Extension in the Tyrrhenian Sea and shortening in the Apennines as result of arc migration driven by sinking of the lithosphere. *Tectonics*, 5(2), 227–245. Available from: https://doi.org/10.1029/TC005i002p00227

Mastrolembo Ventura, B., Serpelloni, E., Argnani, A., Bonforte, A., Bürgmann, R., Anzidei, M. et al. (2014) Fast geodetic strain-rates in eastern Sicily (southern Italy): new insights into block tectonics and seismic potential in the area of the great 1693 earthquake. *Earth and Planetary Science Letters*, 404, 77–88. Available from: https://doi.org/10.1016/j.epsl.2014.07.025

Meschis, M., Roberts, G. P., Mildon, Z. K., Robertson, J., Michetti, A. M. & Faure Walker, J. P. (2019) Slip on a mapped normal fault for the 28th December 1908 Messina earthquake (Mw 7.1) in Italy. *Scientific Reports*, 9(1), 6481. Available from: https://doi.org/10.1038/s41598-019-42915-2

Meschis, M., Roberts, G.P., Robertson, J. & Briant, R.M. (2018) The relationships between regional quaternary uplift, deformation across active Normal faults, and historical seismicity in the upper plate of subduction zones: the capo D'Orlando fault, NE Sicily. *Tectonics*, 37(5), 1231–1255. Available from: https://doi.org/10.1029/2017TC004705

Meschis, M., Roberts, G.P., Robertson, J., Mildon, Z.K., Sahy, D., Goswami, R. et al. (2022a) Out of phase quaternary uplift-rate changes reveal normal fault interaction, implied by deformed marine palaeoshorelines. *Geomorphology*, 416, 108432. Available from: https://doi.org/10.1016/j.geomorph.2022.108432 [online] Available from: https://linkinghub.elsevier.com/retrieve/pii/S0169555X22003257

Meschis, M., Scicchitano, G., Roberts, G.P., Robertson, J., Barreca, G., Monaco, C. et al. (2020) Regional deformation and offshore crustal

local faulting as combined processes to explain uplift through time constrained by investigating differentially-uplifted Late Quaternary palaeoshorelines: the foreland Hyblean plateau, SE Sicily. *Tectonics*, 39(12), Available from: https://doi.org/10.1029/2020TC006187

Meschis, M., Teza, G., Serpelloni, E., Elia, L., Lattanzi, G., Di Donato, M. et al. (2022b) Refining rates of active crustal deformation in the upper plate of subduction zones, implied by geological and geodetic data: the E-dipping west Crati fault, southern Italy. *Remote Sensing*, 14(21), 5303. Available from: https://doi.org/10.3390/rs14215303 [online] Available from: https://www.mdpi.com/2072-4292/14/21/5303

Mildon, Z.K., Roberts, G.P., Faure Walker, J.P., Beck, J., Papanikolaou, I., Michetti, A.M. et al. (2022) Surface faulting earthquake clustering controlled by fault and shear-zone interactions. *Nature Communications*, 13(1), 7126. Available from: https://doi.org/10.1038/s41467-022-34821-5 [online] Available from: https://www.nature.com/articles/s41467-022-34821-5

Miller, W.R. & Mason, T.R. (1994) Erosional features of coastal Beachrock and Aeolianite outcrops in Natal and Zululand, South Africa. *Journal of Coastal Research*, 10, 374–394. Available from: https://doi.org/10.2307/4298223

Miyauchi, T., Dai Pra, G. & Sylos, L.S. (1994) Geochronology of Pleistocene marine terraces and regional tectonics in the Tyrrhenian coast of South Calabria, Italy. *Il Quaternario*, 7, 17–34.

Monaco, C. & Tortorici, L. (2000) Active faulting in the Calabrian arc and eastern Sicily. *Journal of Geodynamics*, 29(3-5), 407–424. Available from: https://doi.org/10.1016/S0264-3707(99)00052-6 [online] Available from: http://linkinghub.elsevier.com/retrieve/pii/S0264370799000526

Neri, G., Barberi, G., Oliva, G. & Orecchio, B. (2005) Spatial variations of seismogenic stress orientations in Sicily, South Italy. *Physics of the Earth and Planetary Interiors*, 148(2-4), 175–191. Available from: https://doi.org/10.1016/j.pepi.2004.08.009 [online] Available from: https://linkinghub.elsevier.com/retrieve/pii/S0031920104003127

Neri, G., Marotta, A.M., Orecchio, B., Presti, D., Totaro, C., Barzaghi, R. et al. (2012) How lithospheric subduction changes along the Calabrian arc in southern Italy: geophysical evidences. *International Journal of Earth Sciences*, 101(7), 1949–1969. Available from: https://doi.org/10.1007/s00531-012-0762-7

Ott, R.F., Gallen, S.F., Wegmann, K.W., Biswas, R.H., Herman, F. & Willett, S.D. (2019) Pleistocene terrace formation, quaternary rock uplift rates and geodynamics of the Hellenic subduction zone revealed from dating of paleoshorelines on Crete, Greece. *Earth and Planetary Science Letters*, 525, 115757. Available from: https://doi.org/10.1016/j.epsl.2019.115757

Palano, M., Ferranti, L., Monaco, C., Mattia, M., Aloisi, M., Bruno, V. et al. (2012) GPS velocity and strain fields in Sicily and southern Calabria, Italy: updated geodetic constraints on tectonic block interaction in the Central Mediterranean. *Journal of Geophysical Research - Solid Earth*, 117(B7), 1–12. Available from: https://doi.org/10.1029/2012JB009254

Palano, M., Piromallo, C. & Chiarabba, C. (2017) Surface imprint of toroidal flow at retreating slab edges: the first geodetic evidence in the Calabrian subduction system. *Geophysical Research Letters*, 44(2), 845–853. https://agupubs.onlinelibrary.wiley.com/doi/10.1002/2016GL071452

Palano, M., Schiavone, D., Loddo, M., Neri, M., Presti, D., Quarto, R. et al. (2015) Active upper crust deformation pattern along the southern edge of the Tyrrhenian subduction zone (NE Sicily): insights from a multidisciplinary approach. *Tectonophysics*, 657, 205–218. Available from: https://doi.org/10.1016/j.tecto.2015.07.005 [online] Available from: https://linkinghub.elsevier.com/retrieve/pii/S0040195115003716 (Accessed 21 May 2024).

Pavano, F., Pazzaglia, F.J. & Catalano, S. (2016) Knickpoints as geomorphic markers of active tectonics: a case study from northeastern Sicily (southern Italy). *Lithosphere*, 8(6), 633–648. Available from: https://doi.org/10.1130/L577.1 [online] Available from: https://pubs.geoscienceworld.org/lithosphere/article/8/6/633-648/196537

Pedoja, K., Jara-Muñoz, J., de Gelder, G., Robertson, J., Meschis, M., Fernandez-Blanco, D. et al. (2018) Neogene-quaternary slow coastal uplift of Western Europe through the perspective of sequences of strandlines from the Cotentin peninsula (Normandy, France). *Geomorphology*, 303, 338–356. Available from: https://doi.org/10.1016/j.geomorph.2017.11.021

Piña-Valdés, J., Socquet, A., Beauval, C., Doin, M., D'Agostino, N. & Shen, Z. (2022) 3D GNSS velocity field sheds light on the deformation mechanisms in Europe: effects of the vertical crustal motion on the distribution of seismicity. *Journal of Geophysical Research - Solid Earth*, 127, e2021JB023451. https://agupubs.onlinelibrary.wiley.com/doi/10.1029/2021JB023451

Pondrelli, S., Piromallo, C. & Serpelloni, E. (2004) Convergence vs. retreat in southern Tyrrhenian Sea: insights from kinematics. *Geophysical Research Letters*, 31(6). http://doi.wiley.com/10.1029/2003GL019223

Roberts, G.P., Houghton, S.L., Underwood, C., Papanikolaou, I., Cowie, P.A., Van Calsteren, P. et al. (2009) Localization of quaternary slip rates in an active rift in 105 years: an example from Central Greece constrained by 234U- 230Th coral dates from uplifted paleoshorelines. *Journal of Geophysical Research - Solid Earth*, 114, 1–26. Available from: https://doi.org/10.1029/2008JB005818

Roberts, G.P., Meschis, M., Houghton, S., Underwood, C. & Briant, R.M. (2013) The implications of revised quaternary palaeoshoreline chronologies for the rates of active extension and uplift in the upper plate of subduction zones. *Quaternary Science Reviews*, 78, 169–187. Available from: https://doi.org/10.1016/j.quascirev.2013.08.006 [online] Available from: http://linkinghub.elsevier.com/retrieve/pii/S0277379113003053

Robertson, J., Meschis, M., Roberts, G.P., Ganas, A. & Gheorghiu, D.M. (2019) Temporally constant quaternary uplift rates and their relationship with extensional upper-plate faults in South Crete (Greece), constrained with ^{36}Cl cosmogenic exposure dating. *Tectonics*, 38(4), 1189–1222. Available from: https://doi.org/10.1029/2018TC005410

Robertson, J., Roberts, G.P., Ganas, A., Meschis, M., Gheorghiu, D.M. & Shanks, R.P. (2023) Quaternary uplift of palaeoshorelines in south-western Crete: the combined effect of extensional and compressional faulting. *Quaternary Science Reviews*, 316, 108240. Available from: https://doi.org/10.1016/j.quascirev.2023.108240 [online] Available from: https://linkinghub.elsevier.com/retrieve/pii/S0277379123002883 (Accessed 8 September 2023).

Robertson, J., Roberts, G.P., Iezzi, F., Meschis, M., Gheorghiu, D.M., Sahy, D. et al. (2020) Distributed normal faulting in the tip zone of the south Alkyonides fault system, gulf of Corinth, constrained using 36Cl exposure dating of late-Quaternary wave-cut platforms. *Journal of Structural Geology*, 136, 104063. Available from: https://doi.org/10.1016/j.jsg.2020.104063

Rohling, E.J., Foster, G.L., Grant, K.M., Marino, G., Roberts, A.P., Tamisiea, M.E. et al. (2014) Sea-level and deep-sea-temperature variability over the past 5.3 million years. *Nature*, 508(7497), 477–482. Available from: https://doi.org/10.1038/nature13230

Romano, D., Sabatino, G., Magazù, S., Di Bella, M., Tripodo, A., Gattuso, A. et al. (2023) Distribution of soil gas radon concentration in North-Eastern Sicily (Italy): hazard evaluation and tectonic implications. *Environmental Earth Sciences*, 82(11), 273. https://link.springer.com/10.1007/s12665-023-10956-6

Rovida, A., Locati, M., Camassi, R., Lolli, B. & Gasperini, P. (2020) The Italian earthquake catalogue CPTI15. *Bulletin of Earthquake Engineering*, 18(7), 2953–2984. http://link.springer.com/10.1007/s10518-020-00818-y

Rust, D. & Kershaw, S. (2000) Holocene tectonic uplift patterns in north-eastern Sicily: evidence from marine notches in coastal outcrops. *Marine Geology*, 167(1-2), 105–126. Available from: https://doi.org/10.1016/S0025-3227(00)00019-0 [online] Available from: https://linkinghub.elsevier.com/retrieve/pii/S0025322700000190

Saillard, M., Hall, S.R., Audin, L., Farber, D.L., Hérail, G., Martinod, J. et al. (2009) Non-steady long-term uplift rates and Pleistocene marine terrace development along the Andean margin of Chile (31° S) inferred from 10 be dating. *Earth and Planetary Science Letters*, 277(1-2), 50–63. Available from: https://doi.org/10.1016/j.epsl.2008.09.039

Scicchitano, G., Spampinato, C.R., Ferranti, L., Antonioli, F., Monaco, C., Capano, M. et al. (2011) Uplifted Holocene shorelines at capo Milazzo (NE Sicily, Italy): evidence of co-seismic and steady-state deformation. *Quaternary International*, 232(1-2), 201–213. Available from: https://doi.org/10.1016/j.quaint.2010.06.028

Serpelloni, E., Anzidei, M., Baldi, P., Casula, G. & Galvani, A. (2005) Crustal velocity and strain-rate fields in Italy and surrounding regions: new results from the analysis of permanent and non-permanent GPS networks. *Geophysical Journal International*, 161(3), 861–880. Available from: https://doi.org/10.1111/j.1365-246x.2005.02618.x

Serpelloni, E., Bürgmann, R., Anzidei, M., Baldi, P., Mastrolembo Ventura, B. & Boschi, E. (2010) Strain accumulation across the Messina Straits and kinematics of Sicily and Calabria from GPS data and dislocation modeling. *Earth and Planetary Science Letters*, 298(3-4), 347–360. Available from: https://doi.org/10.1016/j.epsl.2010.08.005 [online] Available from: http://linkinghub.elsevier.com/retrieve/pii/S0012821X10005157

Serpelloni, E., Faccenna, C., Spada, G., Dong, D. & Williams, S.D.P. (2013) Vertical GPS ground motion rates in the Euro-Mediterranean region: new evidence of velocity gradients at different spatial scales along the Nubia-Eurasia plate boundary. *Journal of Geophysical Research - Solid Earth*, 118(11), 6003–6024. http://doi.wiley.com/10.1002/2013JB010102

Siddall, M., Rohling, E.J., Almogi-Labin, A., Hemleben, C., Meischner, D., Schmelzer, I. et al. (2003) Sea-level fluctuations during the last glacial cycle. *Nature*, 423(6942), 853–858. Available from: https://doi.org/10.1038/nature01690

Stein, R.S. & Barrientos, S.E. (1985) Planar high-angle faulting in the basin and range: geodetic analysis of the 1983 Borah peak, Idaho, earthquake. *Journal of Geophysical Research*, 90(B13), 11355–11366. http://doi.wiley.com/10.1029/JB090iB13p11355.

Stewart, I.S., Cundy, A., Kershaw, S. & Firth, C. (1997) Holocene coastal uplift in the taormina area, northeastern sicily: implications for the southern prolongation of the calabrian seismogenic belt. *Journal of Geodynamics*, 24(1-4), 37–50. Available from: https://doi.org/10.1016/S0264-3707(97)00012-4 [online] Available from: http://linkinghub.elsevier.com/retrieve/pii/S0264370797000124

Tarquini, S., Vinci, S., Favalli, M., Doumaz, F., Fornaciai, A. & Nannipieri, L. (2012) Release of a 10-m-resolution DEM for the Italian territory: comparison with global-coverage DEMs and anaglyph-mode exploration via the web. *Computers & Geosciences*, 38(1), 168–170. Available from: https://doi.org/10.1016/j.cageo.2011.04.018 [online] Available from: http://www.sciencedirect.com/science/article/pii/S0098300411001609 (Accessed 17 February 2016).

Tortorici, G., Bianca, M., De Guidi, G., Monaco, C. & Tortorici, L. (2003) Fault activity and marine terracing in the capo Vaticano area (southern Calabria) during the middle-Late Quaternary. *Quaternary International*, 101–102, 269–278. Available from: https://doi.org/10.1016/S1040-6182(02)00107-6 [online] Available from: http://linkinghub.elsevier.com/retrieve/pii/S1040618202001076

Valensise, G. & Pantosti, D. (1992) A 125 Kyr-long geological record of seismic source repeatability: the Messina Straits (southern Italy) and the 1908 earthquake (M s 7/2). *Terra Nova*, 4(4), 472–483. http://doi.wiley.com/10.1111/j.1365-3121.1992.tb00583.x

Ward, S.N. & Valensise, G. (1989) Fault parameters and slip distribution of the 1915 Avezzano, Italy, earthquake derived from geodetic observations. *Bulletin of the Seismological Society of America*, 79(3), 690–710. Available from: https://doi.org/10.1785/BSSA0790030690

Westaway, R. (1993) Quaternary uplift of southern Italy. *Journal of Geophysical Research*, 98(B12), 741–772. http://www.agu.org/pubs/crossref/1993/93JB01566.shtml

SUPPORTING INFORMATION

Additional supporting information can be found online in the Supporting Information section at the end of this article.